Regulation of spermatogenesis by a local functional axis in the testis: role of the basement membrane–derived noncollagenous 1 domain peptide

Haiqi Chen,* Dolores D. Mruk,* Will M. Lee,[†] and C. Yan Cheng[*,†,1]

*The Mary M. Wohlford Laboratory for Male Contraceptive Research, Center for Biomedical Research, Population Council, New York, New York, USA; and [†]School of Biological Sciences, University of Hong Kong, Pokfulam, Hong Kong, China

ABSTRACT: Spermatogenesis takes place in the epithelium of the seminiferous tubules of the testes, producing millions of spermatozoa per day in an adult male in rodents and humans. Thus, multiple cellular events that are regulated by an array of signaling molecules and pathways are tightly coordinated to support spermatogenesis. Here, we report findings of a local regulatory axis between the basement membrane (BM), the blood-testis barrier (BTB), and the apical ectoplasmic specialization (apical ES; a testis-specific, actin-rich adherens junction at the Sertoli cell–spermatid interface) to coordinate cellular events across the seminiferous epithelium during the epithelial cycle. In short, a biologically active fragment, noncollagenous 1 (NC1) domain that is derived from collagen chains in the BM, was found to modulate cell junction dynamics at the BTB and apical ES. NC1 domain from the collagen α3(IV) chain was cloned into a mammalian expression vector, pCI-neo, with and without a collagen signal peptide. We also prepared a specific Ab against the purified recombinant NC1 domain peptide. These reagents were used to examine whether overexpression of NC1 domain with high transfection efficacy would perturb spermatogenesis, in particular, spermatid adhesion (*i.e.,* inducing apical ES degeneration) and BTB function (*i.e.,* basal ES and tight junction disruption, making the barrier leaky), in the testis *in vivo*. We report our findings that NC1 domain derived from collagen α3(IV) chain—a major structural component of the BM—was capable of inducing BTB remodeling, making the BTB leaky in studies *in vivo*. Furthermore, NC1 domain peptide was transported across the epithelium *via* a microtubule-dependent mechanism and is capable of inducing apical ES degeneration, which leads to germ cell exfoliation from the seminiferous epithelium. Of more importance, we show that NC1 domain peptide exerted its regulatory effect by disorganizing actin microfilaments and microtubules in Sertoli cells so that they failed to support cell adhesion and transport of germ cells and organelles (*e.g.,* residual bodies, phagosomes) across the seminiferous epithelium. This local regulatory axis between the BM, BTB, and the apical ES thus coordinates cellular events that take place across the seminiferous epithelium during the epithelial cycle of spermatogenesis.—Chen, H., Mruk, D. D., Lee, W. M., Cheng, C. Y. Regulation of spermatogenesis by a local functional axis in the testis: role of the basement membrane–derived noncollagenous 1 domain peptide. FASEB J. 31, 3587–3607 (2017). www.fasebj.org

KEY WORDS: Sertoli cell · collagen · NC1 domain · ectoplasmic specialization · blood-testis barrier

In the mammalian testis, basement membrane (BM), a modified form of the extracellular matrix and a product of Sertoli and peritubular myoid cells (1, 2), is mostly constituted by type IV collagen, laminins (*e.g.,* laminin α1, α2, β1, β2, γ1), heparin sulfate proteoglycan, and nidogen (formerly called entactin) (3–5). As BM is in direct contact with Sertoli cells in the seminiferous epithelium, it is likely that there are crosstalks between Sertoli cells and the BM by which BM modulates Sertoli cell function. Indeed, studies *in vitro* have shown that BM modulates Sertoli cell differentiation, Sertoli cell barrier function, and germ cell development (6–8). Studies in rats have also shown that a disruption of the BM function—for instance, by passive transfer of Abs raised against seminiferous tubule BM— leads to focal sloughing of the seminiferous epithelium (9, 10), which illustrates that the BM is necessary to support spermatogenesis. Furthermore, exposure of Sertoli cells cultured *in vitro* with an established functional tight junction (TJ)-permeability barrier to an Ab against type IV collagen (collagen IV) was found to perturb the TJ barrier

function (11), which illustrates the role of collagen at the BM in Sertoli cell function.

Type IV collagen is a triple helical structure that consists of 3 α chains of α1(IV) to α6(IV) in rodent testes, with collagen α3(IV) being the most predominant chain in the testis in which 3 collagen α3(IV) chains constitute a monomer, the building block of the collagen network in the BM (12–15). Each collagen chain is composed of an N-terminal noncollagenous 7S domain of ~15 aa residues, a middle collagenous domain of ~1400 residues of G-X-Y repeats, and a C-terminal noncollagenous 1 (NC1) domain of ~230 aa (4). Collagens are scaffolding proteins that provide structural support to epithelial cells and endothelial cells, but emerging evidence has shown that NC1 fragments of collagen chains generated by limited proteolysis *via* the action of matrix metalloproteinases (MMPs), such as MMP-9, are physiologically active peptides (16). In fact, studies have shown that collagen IV and XVIII chains in the BM of endothelia and epithelia are capable of releasing different biologically active fragments from the NC1 domain: tumstatin, endostatin, arresten, canstatin, hexastatin, and tetrastatin, which are generated endogenously *via* the action of MMPs and are shown to inhibit angiogenesis and tumor growth as well as modulate cell adhesion, proliferation, and apoptosis *via* interactions with cell-surface integrin receptors (16–29). An earlier report that used Sertoli cells cultured *in vitro* coupled with immunohistochemistry using cross-sections of rat testes showed that TNF-α, which is also produced endogenously in the testis (30), was found to stimulate the production of activated MMP-9, which was likely used to generate NC1 fragment from collagen α3(IV) to modulate the Sertoli cell TJ barrier function (11). Despite these earlier findings, it remains to be investigated whether the NC1 domain of collagen α3(IV) [Colα3(IV) NC1] can modulate Sertoli and/or germ cell function in the testis during the epithelial cycle of spermatogenesis. Although an earlier study that used recombinant Colα3(IV) NC1 protein showed that inclusion of this recombinant protein in Sertoli cells cultured *in vitro* with an established TJ barrier indeed perturbs the permeability function dose dependently, its effects in the testis *in vivo* and the likely mechanism of action remain unexplored. Here, we sought to perform a detailed *in vitro* and *in vivo* study to examine the function and likely mechanism of action of this Colα3(IV) NC1 protein in modulating spermatogenesis in the testis. These results demonstrate unequivocally the presence of a functional axis between the BM, the basal ectoplasmic specialization (ES)/blood-testis barrier (BTB), and the apical ES across the seminiferous epithelium that is modulated by the Colα3(IV) NC1 domain serving as an autocrine factor.

MATERIALS AND METHODS

Animals

Sprague-Dawley male pups and adults were obtained from Charles River Laboratories (Kingston, NY, USA). Animals were housed at the Rockefeller University Comparative Bioscience Center (New York, NY, USA) with *ad libitum* access to standard rat chow and water, and were maintained according to the *Guide for the Care and Use of Laboratory Animals* [National Institutes of Health (NIH), Bethesda, MD, USA]. Rats were euthanized by CO_2 asphyxiation using slow (20–30%/min) displacement of chamber air with compressed CO_2 in a euthanasia chamber with built-in regulator approved by the Rockefeller University Laboratory Safety and Environmental Health. All experiments that involved the use of animals were approved by Rockefeller University Institutional Animal Care and Use Committee (protocols 12-506 and 15-780-H). Use of recombinant DNA for experiments reported herein was also approved by the Rockefeller University Institutional Biosafety Committee (Approval No. 2-15-04-007).

Abs

Abs used for experiments reported herein were obtained commercially unless otherwise specified (**Table 1**). The working dilutions for different applications, such as immunofluorescence (IF) analysis by fluorescence microscopy or confocal microscopy, immunohistochemistry (IHC), and immunoblotting (IB), are listed in Table 1.

Primary Sertoli cell cultures

Sertoli cells were isolated from 20-d-old rat testes as described (31). Cells were plated on Matrigel-coated (diluted at 1:5 or 1:7; BD Biosciences, San Jose, CA, USA) 6- or 12-well plates, bicameral units, or round cover glasses (18 mm in diameter) at different cell densities optimized for specific experiments on the basis of pilot experiments. For preparation of cell lysates for IB, endocytosis assay, and actin bundling assay, Sertoli cells were plated at 0.3×10^6 cells/cm^2 on 6-well plates that contained 5 ml F12/DMEM that was supplemented with growth factors (insulin, transferrin, epidermal growth factor) and gentamicin (referred to as culture medium). For transepithelial electrical resistance (TER) measurements to monitor the Sertoli cell TJ permeability barrier function, Sertoli cells were plated at 1.2×10^6 cells/cm^2 on Millicell HA cell culture inserts (diameter, 12 mm; 0.45-μm pore size; effective surface area, ~0.6 cm^2; Millipore, Billerica, MA, USA). Bicameral inserts were placed in 24-well plates with each insert containing 0.5 ml media in the apical and basal chambers. For IF or dual-labeled IF analysis, Sertoli cells were cultured at 0.04×10^6 cells/cm^2 on microscopic round cover glasses, which were then placed on 12-well plates with each well containing 2 ml culture medium. For confocal microscopy, Sertoli cells were cultured at 0.8×10^6 cells/cm^2 on Matrigel-coated transwell permeable supports (Costar polyester membrane inserts, 24-mm in diameter, 0.4-μm pore size; Corning, Corning, NY, USA), which were then placed on 6-well dishes with 2 ml F12/DMEM in the apical and basal compartments.

Assessment of Sertoli cell TJ permeability barrier function

TJ permeability barrier function was monitored by quantifying TER across the Sertoli cell epithelium every 24 h as previously described (31, 32). In brief, Sertoli cells were seeded on Matrigel-coated bicameral units at 1.2×10^6 cells/cm^2. Bicameral units were then paced in 24-well plates with 0.5 ml F12/DMEM each in the apical and basal compartments. The experiment was repeated at least 3 times using different batches of Sertoli cells which yielded similar results.

TABLE 1. *Primary Abs used for different experiments in this report*

Ab (RRID)	Host species	Vendor	Catalog no.	Application (dilution)
Actin (AB_630836)	Goat	Santa Cruz Biotechnology	sc-1616	IB (1:200)
Arp3 (AB_476749)	Mouse	Sigma-Aldrich	A5979	IB (1:3000), IF-tissue (1:200), IF-cell (1:50)
α-Tubulin (AB_2241126)	Mouse	Abcam	ab7291	IF (1:500), IHC (1:300)
β1-Integrin (AB_2128200)	Goat	Santa Cruz Biotechnology	sc-6622	IF (1:100)
β-Catenin (AB_138792)	Mouse	Thermo Fisher Scientific	138400	IB (1:300), IF (1:100)
CAR (AB_2087557)	Rabbit	Santa Cruz Biotechnology	sc-15405	IB (1:200)
CAR (AB_2261263)	Goat	Santa Cruz Biotechnology	sc-10313	IF (1:100)
Claudin 11 (AB_2533259)	Rabbit	Thermo Fisher Scientific	36-4500	IB (1:200), IF (1:100)
Col α1(IV) (AB_305584)[a]	Rabbit	Abcam	ab6586	IF (1:200)
Col α3(IV) NC1	Rabbit	C.Y.C. Laboratory (34)		IB (1:300), IF (1:100)
Col α3(IV) (AB_2082655)	Goat	Santa Cruz Biotechnology	sc-18178	IF (1:100)
Eps8 (AB_397544)	Mouse	BD Biosciences	610143	IB (1:5000), IF-tissue (1:100), IF-cell (1:50)
Laminin-γ3	Rabbit	C.Y.C. Laboratory (62)		IF (1:300)
N-Cadherin (AB_2313779)	Mouse	Thermo Fisher Scientific	33-3900	IB (1:200), IF (1:100)
Nectin-2 (AB_2174166)	Goat	Santa Cruz Biotechnology	sc-14802	IF (1:100)
Nectin-3 (AB_2174276)	Goat	Santa Cruz Biotechnology	sc-14806	IF (1:100)
Occludin (AB_2533977)	Rabbit	Thermo Fisher Scientific	711500	IB (1:250)
ZO-1 (AB_2533938)	Rabbit	Thermo Fisher Scientific	61-7300	IB (1:250), IF (1:100)

CAR, coxsackievirus and adenovirus receptor; RRID, Research Resource Identifier. [a]This Ab prepared against the entire collagen α1(IV) chain (1–1669 aa from the N terminus, which was used as the source of antigen) also cross-reacted with collagen α2, α3, α4, α5, and α6 chains [*i.e.*, including collagen α3(IV) chain], but had negligible cross-reactivity with type I, II, III, V, and VI collagens, as noted by the manufacturer, which was also supported by sequence homology comparison between different type IV collagen chains at both the amino acid and nucleotide sequence levels as shown in Supplemental Fig. S1*C*. In addition, studies have shown that collagen α1(IV) and α2(IV) chains are found in nongonadal BM (15), and collagen α3(IV) and α4(IV) chains are the predominant collagen chains in the BM of rodent testes (13). Thus, this Ab likely recognized mostly collagen α3(IV) and α4(IV) in the rat testis shown herein (Supplemental Fig. S1*B* and Fig. 1*C*, top).

Treatment of adult rats with paclitaxel

Adult male rats (~300 g body weight) were treated with paclitaxel (PTX; Taxol) *via* intratesticular injection as described (33). In short, a stock solution of PTX (M_r 853.9; Sigma-Aldrich, St. Louis, MO, USA) was prepared by dissolving 5 mg PTX in 33.3 μl DMSO. For each rat ($n = 6$ per time point), the right testis received 50 μl PBS (vehicle control), whereas the left testis received ~42.7 μg PTX (dissolved in DMSO) diluted in 50 μl PBS *via* intratesticular injection using a 28-gauge needle with a 0.5-ml insulin syringe. The final concentration of PTX in each testis was 30 μM (assuming the volume of an adult testis of ~1.6 ml), which is the dose that has been previously shown to be effective to disrupt microtubule (MT) function (33). At 24 and 36 h after treatment, rats were euthanized by CO_2 asphyxiation. Pilot experiments have shown that treatment of testes with PTX for 36 h had a phenotype indifferent from 24 h. Thus, rats were humanely killed 24 h after PTX treatment. Testes from 3 rats were isolated and snap-frozen in liquid nitrogen immediately. Cross-sections with thicknesses of ~7 μm were obtained in a cryostat at −22°C for tracking localization of NC1 domain and F-actin. Testes from the other 6 rats were prefixed with 4% paraformaldehyde (PFA) in PBS (w/v) at 4°C for 7 d and were then snap-frozen in liquid nitrogen for α-tubulin staining to monitor the organization of MTs.

Transfection of plasmid DNA

Studies in vitro

Rat collagen α3(IV) chain NC1 domain was cloned as previously described (34), which also served as the template to clone pCI-neo/NC1 that contained the putative signal peptide (SP) of rat collagen α3(IV) chain, namely pCI-neo/rat SP (rSP)-NC1. Four sequential overlapping PCRs were performed to add the putative SP (Supplemental Fig. S1) to the 5′ end of NC1 domain clone, including the *Xho*I site with the sense primer and the *Not*I site in the antisense primer at the 3′ end (**Table 2**). This rSP-NC1 cDNA construct was then cloned into the pCI-neo mammalian expression vector (Promega, Madison, WI, USA) at the *Xho*I and *Not*I cloning sites. pCI-neo/rSP-NC1 was confirmed by direct nucleotide sequencing at Genewiz (South Plainfield, NJ, USA). For IB and actin bundling assay, primary Sertoli cells were transfected with plasmid DNA at 0.8 μg/1×10^6 cells using K2 Transfection Reagent (K2 Transfection System; Biontex, Munich, Germany) on d 2 of culture for 14 h. Thereafter, cells were rinsed with F12/DMEM twice and cultured in fresh medium for an additional 36 h (*i.e.*, d 4) to allow recovery. The same transfection regimen was used for TER measurements, except that TER reading was obtained daily from each bicameral unit until d 7, and each treatment group has quadruple bicameral units for each experiment. For IF, Sertoli cells were transfected with plasmid DNA on d 3 for 24 h. An additional 48 h was needed to allow recovery. To confirm successful transfection in overexpressing experiments, plasmid DNA was labeled with Cy3 using a Mirus Label*IT* Tracker Intracellular Nucleic Acid Localization kit (Mirus Bio, Madison, WI, USA) so that positively transfected cells were labeled with red fluorescence.

Studies in vivo

In vivo transfection in testes was performed as previously described (35). In brief, 15 μg plasmid DNA, together with 1.8 μl *in vivo*-jetPEI reagent (PolyPlus-transfection, Illkirch-Graffenstaden, France), were suspended in sterile 5% glucose (wt/vol) at room temperature to a final transfection mix volume of 70 μl for each testis. The right rat testis received 70 μl of transfection mix that contained empty pCI-neo vector *via* intratesticular injection, whereas the left testis received the same volume of transfection mix that contained pCI-neo/NC1 plasmid DNA. The day of transfection was arbitrarily set as d 0. Transfection efficiency was assessed by using pCI-neo/DsRed2 plasmid DNA as described in Wan *et al.* (36). In short, the right

TABLE 2. *Primers used for constructing a signal peptide in the collagen α(IV) NC1 domain (pCI-neo/rSP-NC1)*

Primer orientation/primer number	Primer, 5′–3′
Sense 1	GTGGTTAGCACAAGAATGAGAGGCTTCATCTTCAC
Sense 2	*GCTCCTGGCTGCCCCGC*CTGTGGTTAGCACAAGAAT
Sense 3	TTCTTGGCGCTCCTGCT*GCCTATCCTGTTGCTGCTCCTGGCTGCCCCGC*
Sense 4	CA*CTCGAG*ATGCACTCAGAGACTGCTCCAAGGTTCTTGGCGCTCCTGCT
Antisense	CA*GCGGCCGC*TTAGTGTCTTTTCTTCATGCACACCTG

The nucleotide sequence for the SP of rat collagen α3(IV) chain is: 5'- ATGCACTCAGAGACTGCTCCAAGGTTCTTGGCGCTCCTGCT*GCC-TATCCTGTTGCTGCTCCTGGCTGCCCCG*CCTGTGGTTAGC-3', which was constructed using the 4 sense primers and the antisense primer. Four overlapping PCRs were performed by using sense primer 1 and antisense primer in the first PCR (PCR-i), with Cola3(IV) NC1 cDNA (34) serving as the template, to be followed by sense primer 2 and antisense primer in the second PCR (PCR-ii) using PCR product from PCR-i as the template. Thereafter, sense primer 3 and antisense primer in the third PCR (PCR-iii) used PCR product from PCR-ii as the template. Finally, sense primer 4 and antisense primer in the fourth PCR (PCR-iv) using PCR product from PCR-iii as the template to clone the SP into Cola3(IV) NC1. The restriction sites are *Xho*I (italicized/dotted underlined in sense primer 4) at the 5′ end and *Not*I (italicized/dotted underlined in antisense primer) at the 3′ end. The start and stop codons of ATG and TTA, respectively, are double underlined. Nucleotide sequence was confirmed by direct nucleotide sequencing at Genewiz.

testis of a rat was transfected with pCI-neo empty vector, whereas the left testis received pCI-neo/DsRed2 plasmid DNA. Transfection efficacy was estimated by using 2 approaches. First, after treatment, testes removed from rats that were euthanized by CO_2 asphyxiation 24 h later were rinsed with ice-cold PBS (10 mM sodium phosphate, 0.15 M NaCl, pH 7.4, at 22°C) and fixed in 4% PFA (w/v in PBS) for 7 d before being snap-frozen in liquid nitrogen. Sections (~7 μm) were obtained in a cryostat at −22°C and examined by fluorescence microscopy. Tubules with visible red fluorescence were scored. A randomly selected tubule—at least 100 tubules were scored—with at least 10 aggregates of red fluorescence was considered to be successfully transfected and a total of 3 rat testes were scored (*i.e.*, ~300 tubules). Second, in addition to scoring tubules with DsRed2 to confirm successful transfection, the protein level of NC1 domain in lysates of seminiferous tubules after over-expression was also quantified by IB by using an anti-Col α3(IV) NC1 domain Ab. Seminiferous tubules were obtained from testes as previously described by our laboratory (37, 38), except that these tubules were not subjected to additional culture but were harvested to prepare tubule lysates in a manner similar to the procedure for obtaining testis lysates 24 h after transfection.

BTB integrity assay

BTB integrity was assessed by an *in vivo*–based assay to monitor the ability of an intact BTB to exclude the passage of biotin across the immunologic barrier as previously described (39), with minor modifications from earlier reports (40, 41). In short, adult male rats ($n = 3$ adult rats for each group, 270~300 g body weight) received either pCI-neo empty vector or pCI-neo/NC1 for transfection on d 0 as described above and terminated on d 3, 7, and 50, respectively. For positive control, rats received $CdCl_2$ (3 mg/kg body weight, i.p.), which is known to induce irreversible BTB disruption (42, 43). Before termination at each time point, rats were anesthetized by ketamine HCl (60 mg/kg body weight, i.m.) with xylazine as an analgesic (10 mg/kg body weight, i.m.; Sigma-Aldrich). Testes were exposed by making a small incision of ~1 cm in the scrotum, and 100 μl of 10 mg/ml EZ-Link Sulfo-NHS-LC-Biotin (freshly prepared in PBS that contained 1 mM $CaCl_2$; Thermo Fisher Scientific, Waltham, MA, USA), a membrane-impermeable biotinylation reagent with an M_r of 556.59, was gently loaded under the tunica albuginea *via* a 28-gauge needle. After 30 min, rats were euthanized by CO_2 asphyxiation. Testes were removed immediately and snap-frozen in liquid nitrogen. Frozen cross-sections (10 μm thick) of testes obtained in a cryostat at −22°C were fixed at room temperature

in 4% PFA (in PBS, w/v) for 10 min and stained with Alexa Fluor 555-streptavidin (1:250; Thermo Fisher Scientific) for 30 min. Semiquantitative data were obtained from the BTB integrity assay by calculating the ratio between the distance traveled by biotin (D_{Biotin}) from the BM of the seminiferous tubule *vs.* the radius of that tubule (D_{Radius}) for comparisons between the 2 control groups and the treatment group. For sections of oval-shaped tubules, the radius was the average of the shortest and longest distances.

IF and dual-labeled IF analysis

IF was performed by using corresponding primary Abs (Table 1) as described (35, 39). For F-actin staining, rhodamine- or FITC-conjugated phalloidin (Thermo Fisher Scientific) were used as previously described (35, 39). Nuclei were visualized with DAPI. Cells or tissue sections were examined by using an Olympus BX61 fluorescence microscope with a built-in Olympus DP-71 digital camera, and images were acquired using the Olympus MicroSuite Five software package (v.1224; Olympus, Tokyo, Japan). Images were processed by using Adobe Photoshop for image resizing/cropping and overlay (Adobe, San Jose, CA, USA).

Confocal microscopy

For confocal microscopy, images were obtained by using an inverted Zeiss Laser Scanning Microscope (LSM) LSM 880 with nonlinear optics laser (Zeiss, Jena, Germany) that was equipped with the Zeiss Zen software package at the Bio-imaging Resource Center (Rockefeller University). Optical sections of ~0.8 μm were collected at 0.25-μm intervals along the z axis to obtain image series (*i.e.*, z stack). Fiji (ImageJ; NIH; *https://fiji.sc/*) was used to analyze confocal images and to measure distance.

Endocytosis assay

Endocytosis assay was performed essentially as previously described (44, 45). In brief, Sertoli cells cultured at 0.3×10^6 cells/cm^2 on Matrigel-coated 6-well plates for 2 d were transfected with either empty vector or pCI-neo/NC1 plasmid DNA for 14 h, and cells were then rinsed twice with F12/DMEM to remove transfection reagents and were cultured for 2 additional days. Thereafter, cells were washed twice with ice-cold PBS that contained 1 mM $CaCl_2$ and 0.7 mM $MgCl_2$ (PBS/CM) and were

incubated with 0.5 mg/ml Sulfo-NHS-SS-Biotin (Thermo Fisher Scientific) in PBS/CM at 4°C for 30 min to allow biotinylation of cell-surface proteins. Excess Sulfo-NHS-SS-Biotin was quenched by 50 mM NH_4Cl in PBS/CM at 4°C for 15 min. Sertoli cells were then washed twice with ice-cold PBS/CM and incubated with fresh culture media at 35°C for various time points in a humidified atmosphere with 95% air and 5% CO_2 (v/v) to allow internalization of cell surface biotinylated proteins as endocytosis does not occur at 4°C. At specified time points (0, 5, 10, 20, and 120 min), cells were washed in ice-cold PBS/CM, incubated with a biotin stripping buffer [50 mM sodium 2-mercaptoethanesulfonate in 100 mM Tris/HCl (pH 8.6) that contained 100 mM NaCl and 2.5 mM $CaCl_2$] at 4°C for 30 min to remove any remaining biotin or nonendocytosed biotin on the cell surface, and subsequently quenched with a quenching buffer (5 mg/ml iodoacetamide in PBS/CM) at 4°C for 15 min. Cells were then washed twice with ice-cold PBS/CM and lysed in RIPA buffer [50 mM Tris, pH 7.4, at 22°C, that contained 0.15 M NaCl, 2 mM EGTA, 1% NP-40 (v/v), 0.1% SDS (w/v) freshly supplemented with protease and phosphatase inhibitors]. Equal amounts of cell lysates (~400 µg protein) from samples within an experimental set (except for control groups in which only 1/5 of the amount was used to avoid protein overloading for positive control) were incubated with NeutrAvidin beads (Thermo Fisher Scientific) to pull down biotinylated proteins. Beads were washed 4 times in RIPA buffer that was freshly supplemented with protease and phosphatase inhibitors. Biotinylated proteins were extracted in SDS sample buffer [0.125 M Tris, pH 6.8, at 22°C, that contained 1% SDS (w/v), 1.6% 2-mercaptoethanol (v/v), and 20% glycerol (v/v)] for SDS-PAGE, and IB analysis was performed by using corresponding specific Abs (Table 1). Total biotinylated proteins that were obtained in cell lysates without being subjected to treatment with stripping buffer served as positive control. Lysates from cells that were incubated with PBS/CM instead of Sulfo-NHS-SS-Biotin served as negative control. Duplicate wells were used for each time point.

Actin bundling assay

Actin bundling assay was performed essentially as previously described (46, 47). In brief, cell lysates were obtained from Sertoli cells that were transfected with pCI-neo/NC1 plasmid DNA *vs.* pCI-neo (vector alone, control) DNA by using 100 µl lysis buffer [20 mM Tris, 20 mM NaCl and 0.5% Triton X-100 (v/v), pH 7.5, at 22°C, freshly supplemented with protease and phosphatase inhibitors]. A 21-µM F-actin stock solution was prepared by converting G-actin to actin microfilaments for 1 h by using a kit from Cytoskeleton (Denver, CO, USA) according to the manufacturer's instructions. Thereafter, equal amounts of protein from control and treatment groups and 10 µl Tris lysis buffer (serving as negative control) were added to 40 µl of freshly prepared F-actin–containing solution, respectively. These mixtures were incubated for 30 min at room temperature to allow actin bundling, and actin filament bundles were subsequently obtained by centrifugation at 12,000 *g* at 24°C for 5 min. Bundled F-actin was concentrated in the pellet, whereas unbundled actin microfilaments remained in the supernatant. Whole pellet (dissolved in 30 µl MilliQ water) and an aliquot (5 µl) of supernatant from each sample were analyzed by IB using an anti-actin Ab.

Histologic analysis to assess the status of spermatogenesis after NC1 overexpression in adult rat testes

Histologic analysis by using either frozen cross-sections or paraffin-embedded sections were stained by DAPI or hematoxylin and eosin, respectively, was performed as previously described (48). The following parameters were used to characterize seminiferous tubules with defects in the status of spermatogenesis in the testis after overexpression of NC1 domain *vs.* control testes: *1)* germ cell loss in which >15 spermatids/spermatocytes were found within a tubule lumen; *2)* gross changes in the seminiferous epithelium layout, such as a significant reduction in the number of a germ cell type (*e.g.,* elongating/elongated spermatids) in stage VI or VII tubules; *3)* retention of germ cells deep inside the seminiferous epithelium after spermiation had occurred; and *4)* defects in spermatid polarity in which the head of >15 elongating/elongated spermatids no longer pointed toward the BM but deviated by at least 90° from the intended orientation.

Statistical analysis

Each data point was expressed as a mean $\pm$ SD of at least 3 independent experiments or $n = 3$ rats. Statistical significance was evaluated with Student's *t* test for paired comparisons.

RESULTS

Collagen α3(IV) NC1 is expressed at the apical ES in stage VII–VIII tubules

The predominant collagen in the BM of seminiferous tubules is type IV, α3 chain [collagen α3(IV)] (15). Each functional collagen monomer is composed of trimeric collagen α3(IV) chains (**Fig. 1A**), which serve as the building blocks to assemble the collagen network in the BM. Each collagen chain is composed of an N-terminal noncollagenous 7S domain (~15 aa residues), a middle collagenous domain (~1400 residues of G-X-Y repeats), and a C-terminal noncollagenous (NC1) domain (~230 aa), with an apparent M_r of ~170–180 kDa (4). We used an Ab specific to the NC1 domain of collagen α3(IV) chain, which was prepared by using purified recombinant NC1 domain protein as an antigen as previously described (34), with its specificity illustrated by IB using lysates of Sertoli cells (Supplemental Fig. S1A). It was noted that under reducing conditions, this anti-NC1 domain Ab recognized both the NC1 domain peptide (28 kDa) and the collagen α3(IV) chain of ~170–180 kDa (Supplemental Fig. S1A), which demonstrates that the NC1 domain protein is an entity of collagen chain in the testis. Using this anti-NC1 domain Ab, the NC1 domain peptide was detected at the apical ES in the seminiferous epithelium, but only in stage VII and VIII tubules, not the BM, in cross-sections of adult rat testes (Fig. 1B). Using an Abcam (Cambridge, MA, USA) Ab that is specific to human type IV collagen α1 chain (Supplemental Fig. S1B and Table 1) [note that human collagen type IV α1 chain shared extensive sequence similarity with the corresponding rat protein at both the nucleotide and amino acid sequence level and thus cross-reacted with rat α3(IV) chain as noted by the manufacturer; see Supplemental Fig. S1C], collagen α3(IV) [and possibly α4(IV); note that collagen α3(IV) and α4(IV) are the predominant type IV collagen chains found in rodent testes (13)] was detected only near the base of the epithelium, which was consistent with its localization at the BM of the tunica propria (Fig. 1C, upper); however, the anti-NC1 Ab failed
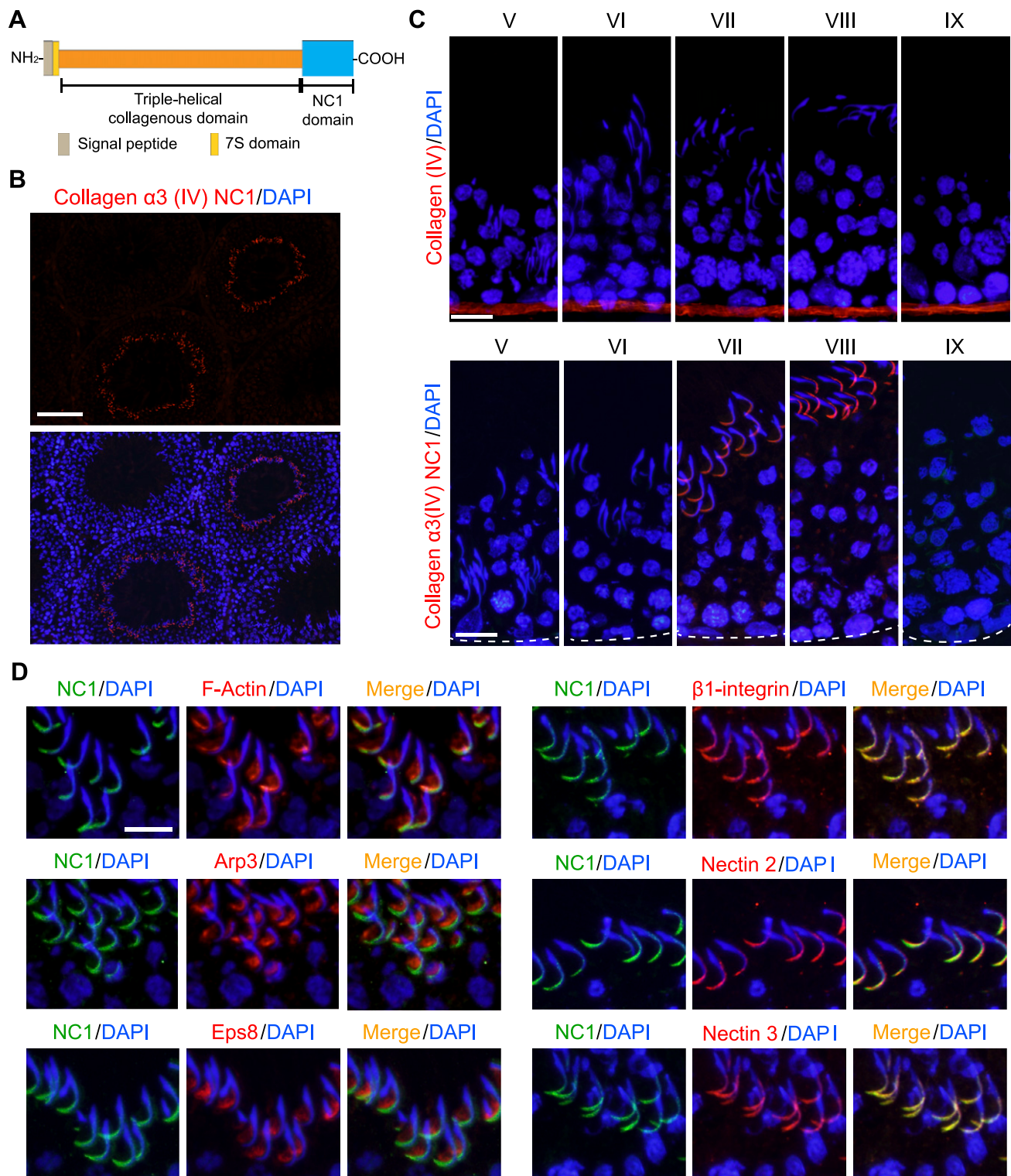
Figure 1. The collagen α3(IV) NC1 domain generated at the BM in the seminiferous epithelium is transported to the apical ES stage specifically. *A*) Schematic that depicts the various functional domains of the collagen α3(IV) chain. Each collagen monomer is a triple-helical structure composed of 3 α chains. The collagen scaffolding function is conferred by a long stretch of Gly-X-X repeats, flanked by an N-terminal 7S domain (behind the signal peptide, which is cleaved before its export from the Sertoli cell), and a C-terminal NC1 domain. *B*) IF analysis using an Ab prepared against the purified recombinant NC1 domain protein [(34); also see Table 1] showed that NC1 was localized near the tip of elongated spermatid heads, consistent with its localization at the apical ES, but restricted to stage VII and VIII tubules. *C*) IF analysis using a rabbit anti-human collagen (IV) Ab from Abcam (Table 1), which also cross-reacted with the rat type IV collagen, including α1 to α6 chains (Supplemental Fig. S1*C*) but not type I, II, III, V, or VI collagens as indicated by the manufacturer. In short, collagen α3(IV) [and also collagen α4(IV); collagen α3(IV) and α4(IV) are the 2 known collagen chains found in the rat testis basement membrane (13)] was localized

to stain the native collagen α3(IV) chain in BM but only stained the apical ES in VII–VIII tubules (Fig. 1C, bottom), perhaps as a result of intrinsic folding of the NC1 domain in the native protein found in the BM *vs.* the NC1 domain peptide at the apical ES as this Ab was prepared by using a recombinant NC1 domain peptide as earlier reported (34). The observation that the localization of the NC1 domain protein at the apical ES was indeed NC1 specific (Fig. 1B, C) was further confirmed by using a commercially available anti-collagen α3(IV) Ab (Santa Cruz Biotechnology, Santa Cruz, CA, USA), which was prepared against the first 51 aa residues of the NC1 domain of human collagen α3(IV) from the N terminus (Table 1 and Supplemental Fig. S1D), which shared extensive identity with rat protein (Supplemental Fig. S1C). Using this specific anti-collagen α3(IV) NC1 domain Ab (Table 1 and Supplemental Fig. S1D), collagen α3(IV) was indeed detected at the basal region, which was consistent with its localization at the BM as well as the apical ES, most prominently at the apical ES in VII–VIII tubules (Supplemental Fig. S1E), which was consistent with findings shown in Fig. 1C (bottom). Collectively, these findings demonstrate unequivocally that the NC1 domain of collagen α3(IV) is a component of the basement membrane, which could be transported across the epithelium from the BM to the apical ES during the epithelial cycle so that it was associated with apical ES in VII–VIII tubules. To further confirm that collagen α3(IV) NC1 domain is a component of the apical ES, dual-labeled IF analysis was performed (Fig. 1D). The NC1 domain protein was localized at the tip of spermatid heads and partially colocalized with F-actin at the apical ES, but not actin regulatory proteins, Arp3 [an actin barbed-end polymerization protein that causes branching of actin microfilaments (49)] or Eps8 [epidermal growth factor receptor pathway substrate 8; an actin bundling and barbed-end capping protein (50); Fig. 1D]; however, the NC1 domain peptide colocalized almost superimposably with apical ES proteins, β1-integrin [specific to Sertoli cells (51)], nectin 3 [specific to spermatids (52)], and nectin 2 [found in both Sertoli cells and spermatids (52); Fig. 1D].

Collagen α3(IV) NC1 domain at the apical ES in stage VII–VIII tubules is transported from the BM *via* an MT-dependent transport mechanism

PTX is a toxicant that is known to block MT-dependent cellular events by stabilizing MTs in mammalian cells, including the testis (33), thereby causing MT disruption. Treatment of the testes with ~30 μM PTX [42.7 μg PTX in 50 μl PBS was administered to the left testis *vs.* PBS alone to the right testis, which served as a control with *n* = 6 rats as described in Russell *et al.* (33)] was found to considerably disrupt the accumulation of NC1 protein at the apical ES in stage VII–VIII tubules *vs.* control testes treated with vehicle (PBS) alone (**Fig. 2A** and Supplemental Fig. S2). These findings thus imply that the considerable reduction of the NC1 domain at the apical ES in PTX-treated testes was a result of a failure of MT-mediated transport. Indeed, there was a gross reduction in the track-like structures conferred by α-tubulin (the building block of MTs; Fig. 2B). For instance, the track-like structures conferred by MTs was grossly disrupted when visualized by α-tubulin staining in testes that were treated with PTX for 24 h (Fig. 2C). This loss of MT function induced by PTX thus diminished the robust expression of the NC1 domain protein at the apical ES at the Sertoli cell-step 19 spermatid interface (Fig. 2D); however, the F-actin–based cytoskeleton was not affected by PTX (Supplemental Fig. S2), which confirmed the notion that only the MT-based transport mechanism was perturbed after PTX treatment.

Overexpression of collagen α3(IV) NC1 in Sertoli cell epithelium perturbs Sertoli cell TJ permeability *via* changes in the localization of TJ and basal ES proteins as the result of an increase in the kinetics of protein endocytosis

We next examined the biologic effects of the NC1 domain on Sertoli cells and the likely underlying signaling mechanisms. In brief, 2 constructs of the NC1 domain with or without the SP of rat collagen α3(IV) chain (rSP) were prepared (**Fig. 3A, B**) by using primer pairs for PCR shown in Table 2 and the NC1 domain cDNA construct previously described (34). Studies have shown that biologically active collagen fragments, such as the NC1 domain, exert their effects *via* integrin receptors, either through outside-in or inside-out signaling (for reviews, see refs. 53–55). Collagen α3(IV) NC1 was cloned into the Mammalian Expression Vector pCI-neo (Promega) as described (34). Furthermore, a signaling peptide of collagen α3(IV) chain shown in Fig. 3B was also cloned into the pCI-neo vector by using specific primer pairs shown in Table 2. Overexpression of the collagen α3(IV) NC1 with

---

restrictively to the base of the seminiferous epithelium, consistent with its localization at the BM (upper); however, NC1 domain stained by an Ab specific to the NC1 domain [prepared in-house using purified recombinant rat collagen α3(IV) NC1 domain (Table 1) as previously characterized (34)] as noted in panel B was found at the apical ES in stage VII–VIII tubules but not in the BM (lower). These findings are consistent with IF data obtained by using a goat anti-collagen α3(IV) Ab from Santa Cruz Biotechnology (Table 1) but against only a stretch of sequence at 1440–1490 aa of collagen α3(IV) at the NC1 domain, which stained almost exclusively to the BM but also the apical ES at stage VII–VIII (with some weak staining at the apical ES at step 9 spermatid-Sertoli cell interface in IX tubules but not other stages; Supplemental Fig. S1). D) Colocalization of NC1 (green fluorescence) with: 1) F-actin (red fluorescence), 2) actin-regulatory proteins Arp3 (red fluorescence, a branched actin polymerization protein that mediates actin barbed-end nucleation), 3) Eps8 (red fluorescence, an actin barbed-end capping and bundling protein), as well as apical ES-specific adhesion proteins 4) β1-integrin (red fluorescence), 5) nectin 2 (red fluorescence), and 6) nectin 3 (red fluorescence) at the apical ES. Cell nuclei were visualized by DAPI (blue fluorescence). Scale bars: 150 μm (A), 20 μm (C, D).
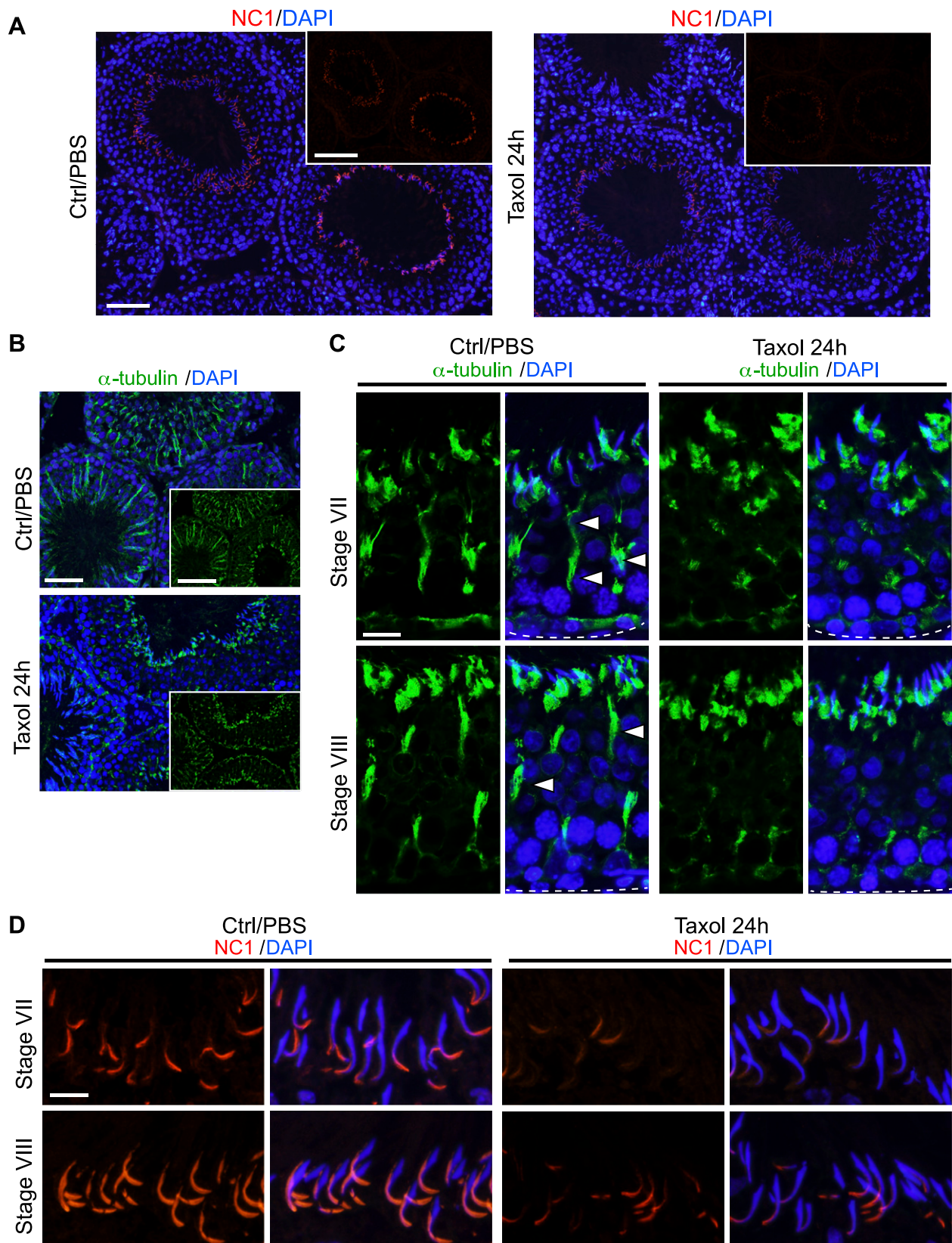
Figure 2. The NC1 domain peptide at the apical ES is transported from the BM *via* a MT-dependent mechanism. *A*) To assess whether NC1 detected at the apical ES is originated from the BM *via* the MT-dependent track-like ultrastructure, testes were treated with PTX (Taxol) as described in Materials and Methods. In control testes, the NC1 domain peptide (red fluorescence) was prominently detected at the apical ES in stage VII–VIII tubules; however, after treatment of testes with PTX for 24 h, NC1 domain peptide was considerably diminished in stage VII–VIII tubules. Scale bars, 80 and 150 µm (inset). *B*) It was noted that treatment of the testes with PTX perturbed MTs to organize into track-like structures to support cellular transports, such as

(*continued on next page*)

(pCI-neo/rSP-NC1) and without the rSP (pCI-neo/NC1) *vs.* vector alone (pCI-neo) was performed on d 2 of Sertoli cell cultures with an established TJ permeability barrier on the basis of analysis of the TJ barrier function and the presence of ultrastructures of TJ, basal ES, and gap junction when visualized by electron microscopy as previously reported (56, 57). Lysates were obtained from these cultures on d 4 for IB. It was noted that overexpression of NC1 was confirmed, wherein an increase of ~50% of the NC1 protein was quantified by IB without affecting steady-state levels of other BTB-associated proteins, including TJ proteins [*e.g.,* coxsackievirus and adenovirus receptor (CAR) and zonula occludens-1 (ZO-1)] and basal ES proteins (*e.g.,* N-cadherin, β-catenin), using β-actin as a protein loading control (Fig. 3*A, C*). Of interest, overexpression of either pCI-neo/NC1 and pCI-neo/rSP-NC1 perturbed the Sertoli cell TJ permeability barrier function (Fig. 3*D*), which demonstrated that NC1 exerted its inhibitory effects either by inside-out or outside-in signaling. In short, the presence of signal peptide rSP is not necessary for NC1 domain to elicit its full biological effect to perturb the Sertoli cell TJ-barrier function based on the findings shown in Fig. 3*D*. Thus, subsequent studies were performed by using pCI-neo/NC1 without the signal peptide. NC1 was found to mediate its TJ barrier disruptive effects *via* changes in the localization of TJ proteins CAR or ZO-1, as well as basal ES proteins N-cadherin or β-catenin when examined by confocal microscopy, whereas these proteins no longer localized closely to the cell-cell interface but diffusely localized at the site (Fig. 3*E*). These findings suggest that an overexpression of the NC1 domain in Sertoli cells would enhance protein endocytosis. A study that used a protein endocytosis assay with CAR as the marker indeed confirmed this notion of an increase in the kinetics of protein endocytosis (Fig. 3*F, G*).

Collagen α3(IV) NC1 domain perturbs the Sertoli cell TJ barrier *via* changes in actin microfilament organization by altering spatial expression of actin regulatory proteins Arp3 and Eps8

We next examined the likely mechanism by which overexpression of the NC1 peptide in Sertoli cell epithelium perturbed the TJ permeability function as shown in Fig. 3*D*. The organization of actin microfilaments across the cell cytosol was grossly affected after overexpression of the NC1 domain in Sertoli cells (**Fig. 4***A*). For instance, actin

microfilaments were truncated and they no longer stretched across the Sertoli cell cytosol as found in control cells, but found mostly at the cell cortical zone (Fig. 4*A*). These changes seemed to be mediated *via* an alteration of the spatial expression of actin barbed-end nucleation protein Arp3 and actin barbed-end capping and bundling protein Eps8 (Fig. 4*A*). Thus, Arp3 and Eps8 effectively caused actin filaments to assume a branched/unbundled and bundled configuration, respectively. However, Arp3 and Eps8 no longer concentrated at the Sertoli cell-cell interface to confer plasticity to the actin microfilament bundles at the Sertoli cell BTB, supporting their remodeling in response to changes in the epithelial cycle. Their disruptive spatial expression thus impeded the proper organization of actin filaments in Sertoli cells (Fig. 4*A*) to support the Sertoli cell TJ barrier function. These findings were noted and confirmed in other experiments when more cells were visualized after NC1 domain overexpression in Sertoli cells (Supplemental Fig. S3). These morphologic findings were further corroborated by biochemical data that were based on a biochemical assay in which the ability of the Sertoli cell lysate to induce actin filament bundling was assessed after overexpression of the NC1 domain was compared with controls (vector alone) *vs.* negative control (buffer alone; Fig. 4*B*). Indeed, a considerable and statistically significant reduction in actin bundling activity was detected in Sertoli cells after overexpression of NC1 domain (Fig. 4*B*).

Overexpression of the collagen α3(IV) NC1 domain in the testis *in vivo* perturbs spermatogenesis

To further confirm the physiologic relevancy of the observations *in vitro*, we next examined changes in the status of spermatogenesis after overexpression of the NC1 domain in the testis *in vivo* using PolyPlus *in vivo*-jetPEI transfection medium, which was recently shown to be suitable for *in vivo* expression of cDNA or RNAi with a high transfection efficiency (39, 58). The efficacy of transfection was estimated by transfecting testes with DsRed2, a *Discosoma sp.* red fluorescence protein, cloned into pCI-neo (pCI-neo/DsRed2) (right testis) *vs.* empty vector (pCI-neo/Ctrl) (left testis) as shown in Supplemental Fig. S4*A* with $n = 3$ rats as previously described (36) on d 0 using PolyPlus *in vivo*-jetPEI transfection medium. Testes were obtained from these rats on d 5 for examination using cross-sections. Fluorescence

---

endocytic vesicles and elongating/elongated spermatids, as virtually no track-like structures were detected in PTX-treated testes. However, the F-actin–based tracks were not perturbed by PTX treatment (Supplemental Fig. S2). Scale bars, 100 and 200 μm (inset). *C*) Magnified micrographs of cross-sections of tubules after PTX treatment *vs.* control testes in stage VII and VIII tubules. The track-like structures (annotated by white arrowheads) conferred by α-tubulin (the building blocks of MTs) were noticeably disrupted after PTX treatment, thereby impeding cellular transport, such as NC1 domain peptide through endocytic vesicles from the BM (annotated by the dashed line). Scale bar, 20 μm. *D*) NC1 (red fluorescence) was seen to localize to the tip of elongated spermatid heads, consistent with its localization at the apical ES in stage VII and VIII tubules in control (normal) testes treated with PBS. Treatment of testes with PTX, however, considerably diminished the amount of NC1 domain at the apical ES, likely the result of a disruption of the MT tracks that support organelle (*e.g.,* NC domain peptide) transport across the seminiferous epithelium. Scale bar, 15 μm.
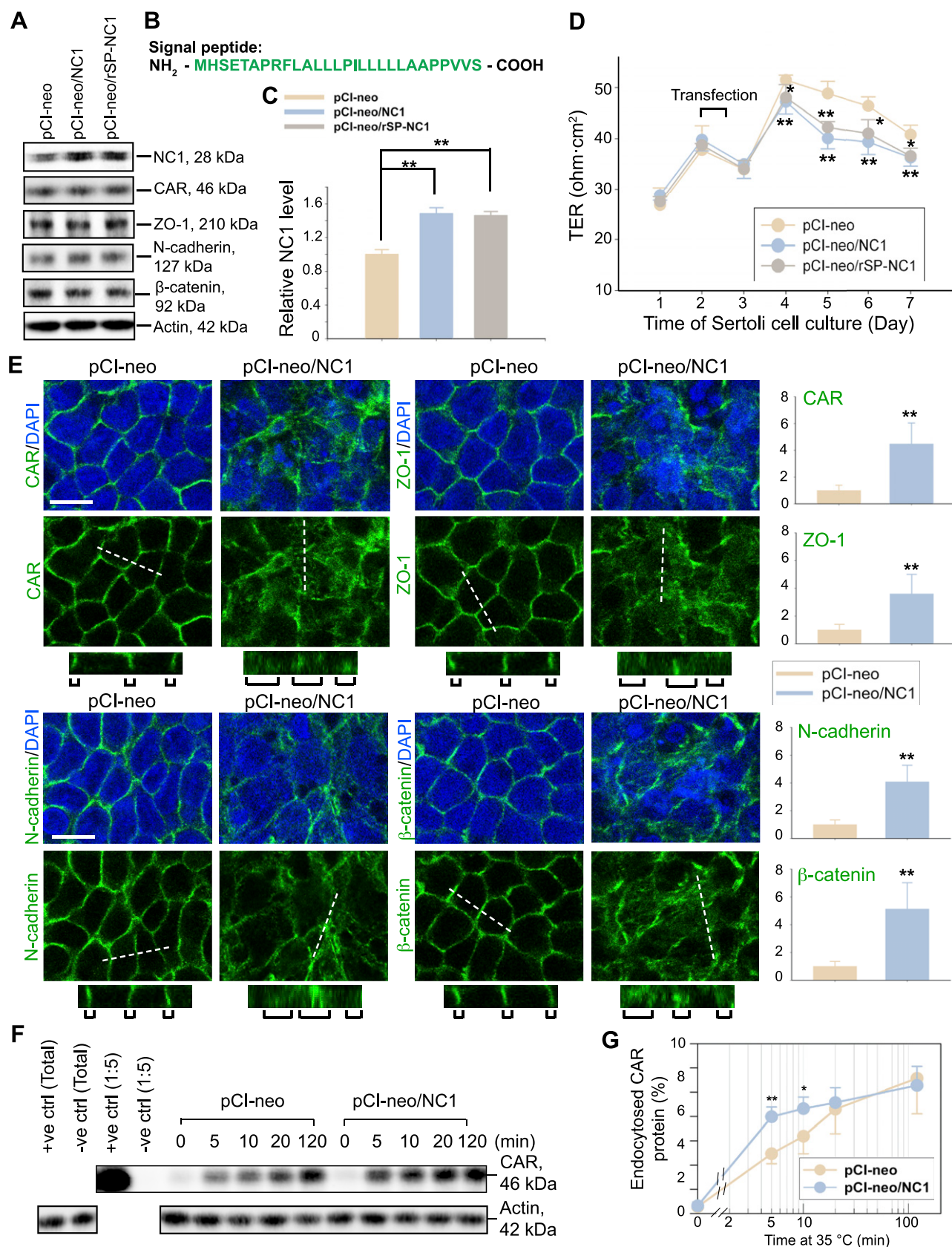
Figure 3. Overexpression of NC1 perturbs Sertoli cell TJ permeability barrier *via* changes in the localization of BTB-associated proteins at the cell-cell interface mediated by a disruption of protein endocytosis kinetics. Sertoli cells were cultured for 2 d to allow the assembly of a functional TJ permeability barrier. Thereafter, cells were transfected with plasmid DNA that contained the construct of either NC1 or NC1 with the SP (rSP-NC1) *vs.* pCI-neo vector alone that served as a control (Ctrl) for 14 h, and lysates were obtained 2 d after transfection (*i.e.,* d 5). *A*) Overexpression of NC1 and NC1 with SP in Sertoli cells (0.3×10^6 cells/cm^2)

(continued on next page)

aggregates of pCI-neo/DsRed2 in ~100 tubules from rat testis of $n = 3$ rats (*i.e.,* 300 tubules total) on d 5 were randomly selected and scored (Supplemental Fig. S4*A*). Successful transfection referred to the cross-section of a tubule that had at least 10 aggregates of red fluorescence (Supplemental Fig. S4*A*). By using this approach, it was estimated that ~60% of scored tubules were positively transfected using PolyPlus *in vivo*-jetPEI transfection medium. Furthermore, the steady-state level of the NC1 domain peptide in testes of rats that were transfected with pCI-neo/NC1 was up-regulated by ~60% when examined by IB analysis on d 2 using lysates obtained from seminiferous tubules that were isolated from these rats (Supplemental Fig. S4*B*). These analyses thus confirmed that overexpression of the NC1 domain peptide in the testis was successful. Overexpression of the NC1 domain (pCI-neo/NC1) in adult rat testes *vs.* control (empty vector, pCI-neo alone; $n = 6$ rats per time point) was found to induce extensive germ cell exfoliation, in particular elongating/elongated spermatids, which was detected on d 5 when transfection was performed at time 0 for 24 h; >60% of tubules were affected, whereas virtually no spermatids were found in the seminiferous epithelium (**Fig. 5**). Of interest, by d 45, elongating/elongated spermatids were found to have begun to repopulate the epithelium, which demonstrated that the NC1 peptide-induced aspermatogenesis was reversible (Fig. 5). It was also noted that on d 3, 5, and 7, some elongating/elongated spermatids were detected in the seminiferous epithelium near the BM, which indicated that some spermatids were persistently trapped deep inside the epithelium of tubules wherein spermiation had occurred. Perhaps this is a result of defects in MT-based tracks that have been recently shown to be crucial to support spermatid transport (59, 60). Interestingly, spermatids residing near the tubule lumen were emptied into the tubule lumen such that virtually no elongating/elongated spermatids were found in the epithelium by d 7 in >80% of the staged V–VIII tubules (Fig. 5). These findings also support the notion that overexpression of the NC1 peptide disrupts F-actin org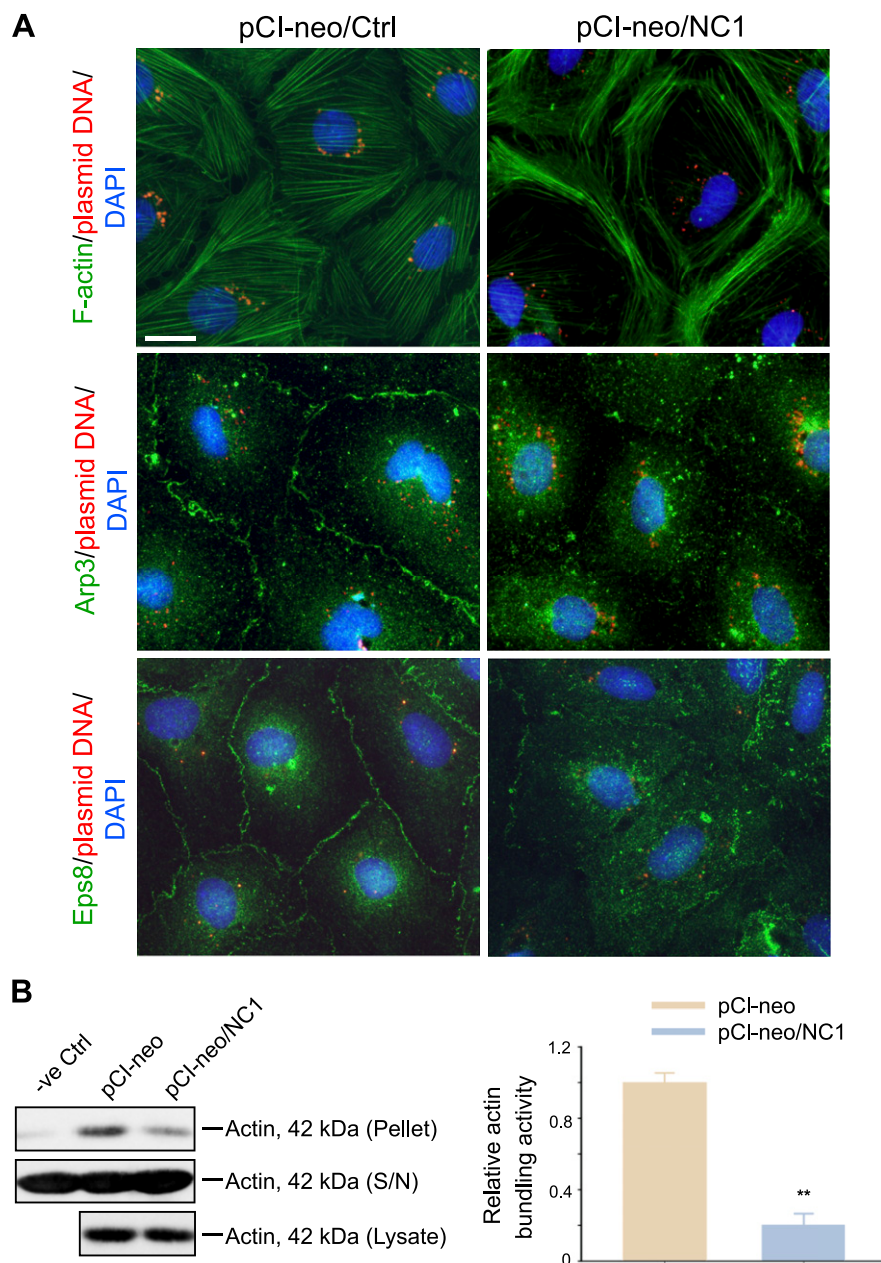anization at the apical ES, which leads to a breakdown of adhesion function at the Sertoli cell-elongating/elongated spermatid interface.

Overexpression of the collagen α3(IV) NC1 domain in the testis *in vivo* perturbs BTB integrity

As the basal ES that contributes to BTB integrity is structurally similar to the apical ES, we next examined whether the BTB in rat testes that were overexpressed with collagen α3(IV) NC1 domain was leaky by using an *in vivo*–based semiquantitative assay. In brief, a membrane-impermeable protein biotinylation reagent Sulfo-NHS-LC-Biotin was loaded (41) under the tunica albuginea, which rapidly diffused into all seminiferous tubules to biotinylate the cell surface proteins as this reagent is water soluble. An intact BTB thus blocked the passage of biotin into the adluminal compartment, but biotin could penetrate a disrupted (*i.e.,* leaky) BTB and labeled proteins in the adluminal (apical) compartment. Thereafter, the presence of biotin was visualized by Alexa Fluor 555-streptavidin (red fluorescence) to assess the integrity of BTB (**Fig. 6**). As noted in the positive control, wherein rats were treated with $CdCl_2$ at 3 mg/kg body weight, i.p.—previously shown to induce irreversible disruption of the BTB (42, 43)—biotin was virtually freely permeable across the BTB to label proteins behind the immunologic barrier, which was in sharp contrast to control (normal) testes in which biotin tracers were blocked from bypassing the BTB (Fig. 6*A*). After overexpression of the NC1 domain in the testis *in vivo*, by d 3, the BTB remained relatively intact; however, it was badly damaged and grossly leaky by d 7, but resealed by d 50 (Fig. 6*A*). These findings were supported by semiquantitative data depicted in Fig. 6*B* when the distance traveled by the biotin trace *vs.* the radius of each tubule (a total of 30 tubules were scored per rat tests with $n = 3$ rats, including the 2 control groups; ~90 tubules were randomly scored; Fig. 6*B*). These analyses thus support the notion that the BTB was reversibly disrupted after overexpression of the NC1 domain in the testis *in vivo*.

---

was confirmed by IB in which the steady-state level of NC1 was found to be induced; however, the levels of other BTB constituent proteins remained unaffected. *B*) Amino acid sequence of the SP of rat collagen a3(IV) chain. Amino acid sequence of collagen α3(IV) chain with the SP and the sequences of the primer pairs used to clone the collagen α3(IV) NC1 domain with the SP are shown in Supplemental Fig. S1 and Table 2, respectively. *C*) Bar graph showing the efficiency of transfection in Sertoli cells, in which transfection of Sertoli cells with the NC1 *vs.* rSP-NC1 cDNA clone led to a ~50% increase in the steady-state level of NC1 in Sertoli cell lysates. Each bar is a mean ± SD of $n = 3$ independent experiments. **$P < 0.01$, Student's *t* test. *D*) Overexpression of NC1 or rSP-NC1 *vs.* pCI-neo DNA (empty vector, Ctrl) was found to perturb the Sertoli cell TJ permeability barrier wherein Sertoli cells (1.2×10^6 cells/cm^2) were cultured on Matrigel-coated bicameral units. Each data point represents a mean ± SD of 4 replicates from a representative experiment, and similar results were obtained from $n = 3$ independent experiments. *E*) Confocal microscopy showing that overexpression of the NC1 domain perturbed the localization of TJ (CAR and ZO-1; green fluorescence) and basal ES (N-cadherin and β-catenin; green fluorescence) proteins at the Sertoli cell-cell interface. These proteins no longer tightly localized at the Sertoli cell BTB, but diffusely localized at the site (*i.e.,* *x-y* plane parallel to the plane of cell attachment). These findings were further confirmed by examining the *x-z* plane (annotated by the dashed line; *i.e.,* perpendicular to the plane of cell attachment; see the third row in each panel). Nuclei were visualized with DAPI (blue fluorescence). Scale bars, 10 μm. Bar graphs in the right panel summarized the analysis of 50 randomly selected cell pairs for each experiment with $n = 3$ experiments that yielded similar results. *F*) Results of a representative endocytosis assay from $n = 3$ independent experiments illustrating overexpression of the NC1 domain peptide in Sertoli cells enhanced the kinetics of endocytosis. The line graph in the right panel confirmed an increase in the rate of endocytosis, which supports the data shown in panel *E*. *$P < 0.05$, **$P < 0.01$ (Student's *t* test compared with corresponding control).

Figure 4. Overexpression of the collagen α3(IV) NC1 domain perturbs the organization of actin filaments *via* changes in spatial expression of actin regulatory proteins Arp3 and Eps8. *A*) F-actin organization was visualized by using FITC-conjugated phalloidin (green fluorescence) in Sertoli cells on d 5 after transfection of corresponding plasmid DNA. Overexpression of the collagen α3(IV) NC1 domain peptide in Sertoli cells led to reorganization of F-actin in which considerably reduced actin microfilaments were found to stretch across the cell cytosol, thereby destabilizing cell adhesion protein complexes that use F-actin for attachment as noted in Fig. 3*E* to support the Sertoli cell TJ barrier function (Fig. 3*D*). As noted herein, these disruptive changes in actin organization were mediated *via* changes in the spatial expression of Arp3 (green fluorescence; a branched actin polymerization protein by inducing a linear actin microfilament to undergo extensive branching) and Eps8 (green fluorescence; an actin barbed-end capping and bundling protein that confers actin filaments to a bundled configuration), whereas Arp3 and Eps8 was no longer highly expressed at the cell-cell interface, but internalized into the cell cytosol. These changes thus contributed to changes in F-actin organization as noted in the top panel. Plasmid DNA was labeled with Cy3 to confirm successful transfection in Sertoli cells. Scale bar, 20 μm. These data were confirmed in other experiments wherein more cells were visualized (Supplemental Fig. S3). *B*) A biochemical assay that monitored the overall actin bundling activity in lysates of Sertoli cells after overexpression of NC1 *vs.* control plasmid DNA. A bar graph on the right panel illustrates the results shown in the left panel in which each bar is a mean ± SD of *n* = 3 experiments, and each experiment had duplicate culture dishes. **$P < 0.01$, Student's *t* test.

Overexpression of the collagen α3(IV) NC1 domain perturbs the organization of actin microfilaments and MTs in the testis

We next examined the mechanism(s) by which over-expression of the NC1 domain peptide induced elongating/elongated spermatid exfoliation and BTB disruption in the testis. First, we sought to investigate whether the actin-based cytoskeleton was impeded, which, in turn, led to spermatid loss and BTB disruption as ES-specific adhesion proteins utilized F-actin for attachment. Indeed, the overall organization of F-actin in the seminiferous epithelium was grossly disrupted by d 5 and 7 after overexpression of the NC1 peptide in the testis *in vivo vs.* control (normal) testes, whereas testes on d 3 remained relatively normal and the actin organization was capable of being re-established by d 45, making the F-actin network similar to control testes (**Fig. 7**). Furthermore, the track-like structures conferred by F-actin that were readily detectable in normal (control) testes—and also by d 45 after overexpression of the NC1 domain peptide—were virtually nondetectable in >80% of tubules examined on d 5 and 7; however, the track-like structures conferred by F-actin by d 3 were only mildly perturbed (Fig. 7), which supported the notion
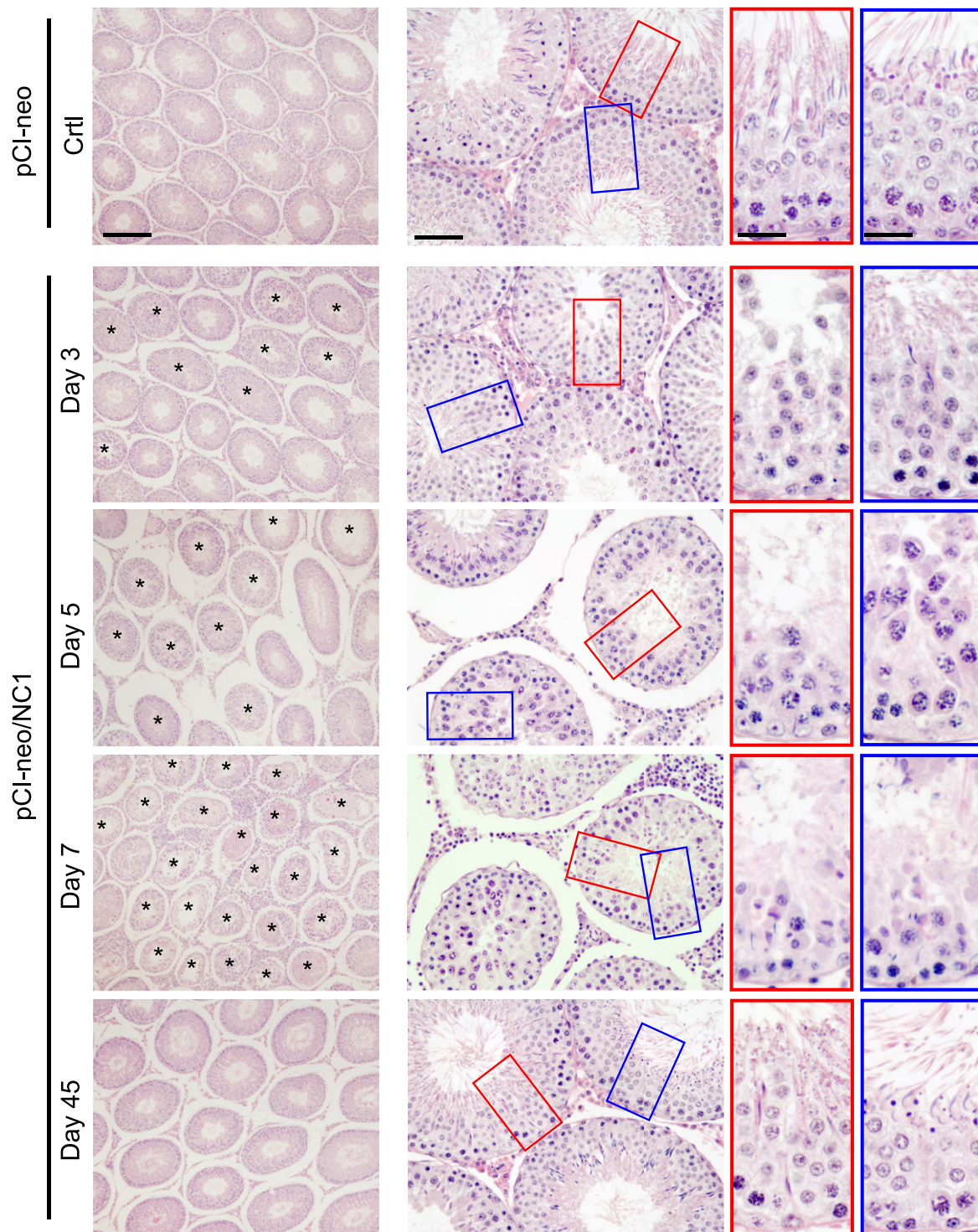
Figure 5. Overexpression of the collagen α3(IV) NC1 domain in the testis *in vivo* reversibly perturbs spermatogenesis. Overexpression of plasmid DNA that contains NC1 domain *vs.* empty vector (ctrl) was performed at time 0, and testes were obtained from rats (*n* = 3 rats for each time point) on d 3, 5, 7, and 45 for histologic analysis after hematoxylin and eosin staining using paraffin-embedded cross-sections of testes. Colored boxes (red or blue) are magnified images to highlight the progressive changes in the premature release of spermatids into the tubule lumen. Asterisks indicate tubules that had obvious defects in spermatogenesis. Premature spermatid loss was detected as earlier as d 3. By d 7, spermatids were no longer found in the majority of tubules; however, some spermatids remained trapped deep inside the seminiferous epithelium in many tubules even though the majority of elongating/elongated spermatids resided near the tubule lumen had undergone spermiation prematurely. Of interest, the status of spermatogenesis was largely restored by d 45, as noted in many of the tubules examined in the testis, illustrating that the disruptive effects of the NC1 domain after its overexpression were reversible. Images shown herein were representative findings of *n* = 3 rats for each time point. Scale bars in first, second, and third and fourth column, 350, 80, and 35 µm, respectively. Transfection efficiency that supported phenotypes shown herein were the result of overexpression of the collagen α3(IV) NC1 domain (conformed by IB) was shown in Supplemental Fig. S4.

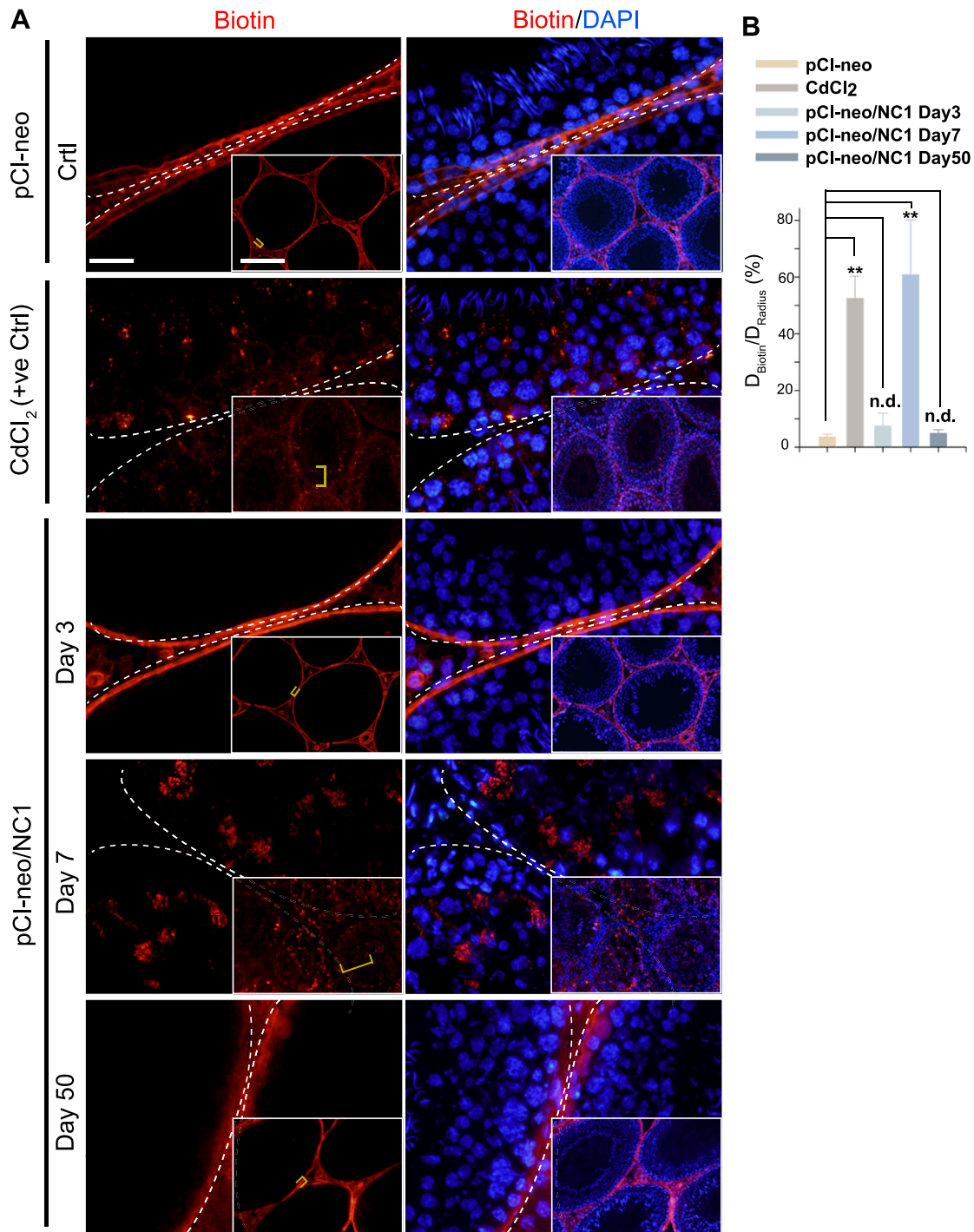**Figure 6.** Overexpression of the collagen α3(IV) NC1 domain in the testis *in vivo* disrupts BTB integrity reversibly. *A)* BTB integrity assay was performed to assess the ability of BTB to block the diffusion of biotin (EZ-Link Sulfo-NHS-LC-Biotin, M_r 556.59, a membrane-impermeable reagent) across the immunologic barrier to enter the adluminal compartment. In testes that were transfected with pCI-neo alone (control, Ctrl), intact BTB blocked biotin (red fluorescence) from entering the adluminal compartment such that red fluorescence was only detected in the basal region of the epithelium and interstitial space. In testes from rats that were treated with $CdCl_2$ (positive control) or after transfection with pCI-neo/NC1 on d 7 (but not d 3), biotin penetrated the BTB and entered the adluminal compartment, illustrating that the BTB was compromised. However, the BTB was resealed by d 50 when the functional BTB blocked the entry of biotin into the adluminal compartment. Distance traveled by biotin beyond the BM/tunica propria (annotated by a dashed white line) is depicted by a yellow bracket. Images of ~3–4 tubules (lower magnification) for each group are shown in the insets and the magnified image of 2 typical tubules is shown in the micrograph. Scale bars, 30 and 250 µm (insets). *B)* Semiquantitative analysis of the findings shown in panel *A* by comparing the distance traveled by biotin (D_{Biotin}) from the BM of the tubule *vs.* the radius of the same tubule (D_{Radius}). These data were summarized in the bar graph with each bar a mean ± SD of ~30 tubules that were randomly selected from testes of 3 rats (from a total of ~90 tubules). For oval-shaped tubules, D_{Radius} is the mean of the longest and shortest distance of the tubule. N.d., not significantly different. *$P < 0.05$, **$P < 0.01$ by Student's *t* test.
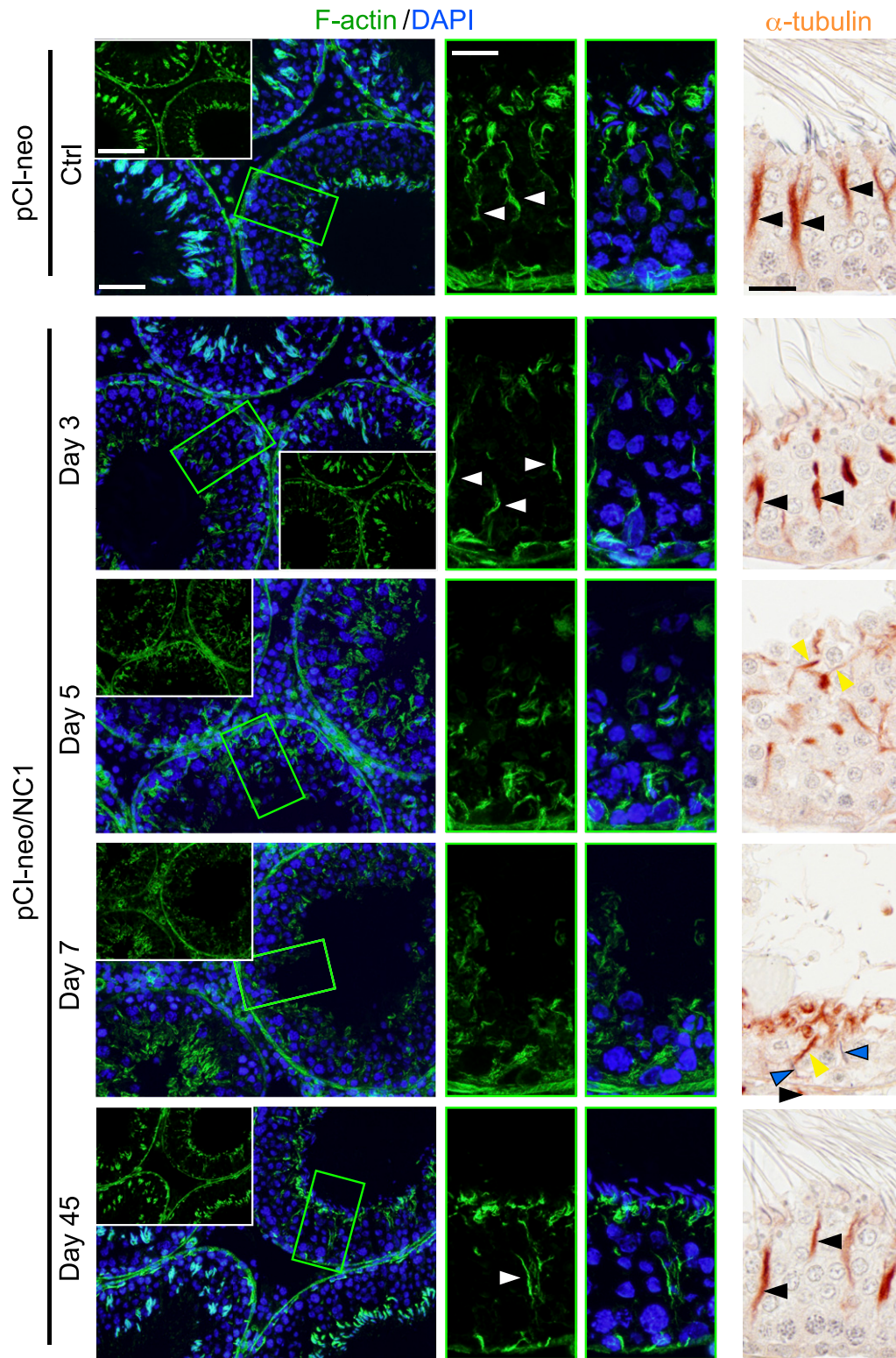
Figure 7. Overexpression of the collagen α3(IV) NC1 domain in the testis *in vivo* alters F-actin and MT organization in the seminiferous epithelium. Rat testes were transfected with pCI-neo/NC1 *vs.* pCI-neo (control) at time 0, and testes were collected at specified time points with *n* = 3 rats for each time point. Frozen sections of testes were used to visualize the organization of F-actin by FITC-phalloidin (green fluorescence). Cell nuclei were visualized by DAPI (blue fluorescence). Overexpression of NC1 led to extensive germ cell exfoliation by d 5 and 7, and F-actin network across the seminiferous epithelium was grossly disrupted at these time points. The typical track-like structures conferred by F-actin (annotated by white arrowheads) at late stage VIII of the epithelial cycle in control testes and also by d 3 were no longer detected in tubules after overexpression of NC1 by d 5 and 7. However, those tracks were restored by d 45 (white arrowhead at the bottom) and germ cells of different classes repopulated the entire epithelium, consistent with data shown in Fig. 6. Green-colored boxes are magnified images to highlight the progressive

that F-actin organization was reversibly disrupted by NC1 domain overexpression. These data are also in agreement with findings, shown in Fig. 5, that by d 3, some of the tubules displayed signs of defects in spermatogenesis as elongated spermatid adhesion was perturbed. In addition, MT-based cytoskeletons were grossly affected by d 5 and 7 after NC1 domain overexpression in the testis, but not in controls and d 45, whereas by d 3, MT organization was mildly perturbed (Fig. 7, right; by immunohistochemistry). These findings are also consistent with disruption of the F-actin network after NC1 domain overexpression in the testis.

Overexpression of the collagen α3(IV) NC1 domain disrupts the apical ES function in the testis *in vivo*

As adhesion protein complexes, such as β1-integrin-laminin-γ3 (61, 62), all utilize F-actin for their attachment at the apical ES, and actin organization at the site is supported by the restrictive spatial expression of Arp3 and Eps8, we examined changes in their expression and/or localization in the testis after overexpression of the NC1 domain peptide. As shown in **Fig. 8**, the organization of F-actin by d 5 was grossly affected, notably perturbed by d 3, and its expression was considerably down-regulated by d 7. For instance, by d 5, F-actin was no longer restricted to the concave (ventral) side of spermatid heads as noted in control testes, and β1-integrin was no longer restrictively expressed at the convex (dorsal) side of spermatid heads (Fig. 8). The mildly affected F-actin organization by d 3 was also reflected by mild changes in localization of Arp3, Eps8, and β1-integrin and laminin-γ3 (Fig. 8). By d 7, expression of β1-integrin and laminin-γ3 was considerably diminished, which was likely a result of the considerable down-regulation of the spatial expression of Arp3 and Eps8 so that F-actin no longer organized to support the adhesion protein complexes at the site. Furthermore, many elongating/elongated spermatids lost their polarity, with their heads no longer pointed toward the BM almost perpendicularly, but deviated by at least 90° from the intended orientation found in control testes (Fig. 8).

Overexpression of the collagen α3(IV) NC1 domain disrupts the basal ES/BTB function in the testis *in vivo*

Similar to the apical ES, the basal ES at the BTB is also an actin-rich ultrastructure, except that it has 2 arrays of actin microfilament bundles, one on each side of the 2 adjacent Sertoli cells *vs.* just a single array of actin bundles on the Sertoli cell side at the Sertoli-spermatid interface (63, 64).

We next examined whether overexpression of the NC1 domain peptide in the testis would impede F-actin organization at the basal ES. Indeed, overexpression of the NC1 domain peptide in the testis *in vivo* led to changes in the organization of F-actin at the basal ES (**Fig. 9A, B**), which, together with actin-based TJ and gap junction, are known to constitute the BTB (63, 65, 66). For instance, F-actin no longer tightly localization at the basal ES as found in control rat testis, but was diffusely localized at the site (Fig. 9) and this disruptive change was notably detected on d 5 and 7, but not on d 3. These data are also consistent with findings shown in Fig. 6 on the basis of the BTB integrity assay. As TJ- (*e.g.*, occludin-ZO-1, claudin 11-ZO-1) and basal ES- (*e.g.*, N-cadherin-β-catenin) associated protein complexes utilize F-actin for their attachment, changes in the organization of F-actin at the basal ES thus impeded the localization of these TJ- and basal ES-associated proteins, whereas they were also diffusely localized at the BTB (Fig. 9A, B). These changes thus impeded BTB integrity, thereby leading to a failure of the BTB to block the diffusion of biotin across the immunologic barrier after overexpression of the NC1 domain peptide (Fig. 9 *vs.* Fig. 6).

DISCUSSION

Spermatogenesis is composed of a series of highly complex cellular events that include *1*) self-renewal of undifferentiated spermatogonia *via* mitosis, *2*) meiosis I/II, *3*) postmeiotic spermatid development *via* spermiogenesis, and *4*) the release of spermatids at spermiation (67, 68). These changes are under precise regulation of the hypothalamic-pituitary-testicular axis and some yet-to-be defined local regulatory mechanisms and/or regulatory molecules (69, 70). It has been reported that at the time of spermiation, biologically active fragments are generated (71), possibly *via* the action of MMP-2, which cleaves laminin-γ3 chains (61) and can serve as autocrine-based factors to induce BTB restructuring (71, 72). Recent studies have identified a peptide, designated F5-peptide, that is generated from the laminin-γ3 chain (73) at the apical ES. This F5-peptide is capable of potentiating apical ES breakdown *via* an autocrine-based mechanism to facilitate the release of sperm at spermiation (39). In addition, this F5-peptide is also capable of inducing BTB remodeling *via* integrin-based inside-out and/or outside-in signaling at the basal ES (72), which is mediated by a disruption on the organization of actin microfilaments and MTs at the basal as well as apical ES (39). These effects thus coordinate the events of spermiation and BTB remodeling that take place simultaneously at the opposite ends of the seminiferous epithelium at stage VIII of the epithelial cycle in the rat testis (64, 73). Studies in the literature have shown that collagen-

changes in the organization of F-actin. MT network in the cross-sections of testes was also visualized by IHC using a tubulin Ag (Table 1), and it was also shown to be disrupted following overexpression of NC1 domain peptide. For instance, the track-like structures conferred by MTs (black arrowheads) noted in Ctrl testes were mildly disrupted by d 3, but grossly affected by d 5 and 7, since they no longer laid perpendicular (yellow arrowheads) to the basement membrane (BM is annotated by the black arrowhead in d 7 testis section). Elongated spermatids (blue arrowheads) were consistently found in tubules embedded deep inside the epithelium by d 7. Interestingly, the MT conferred track-like structures were restored by d 45 (black arrowheads), indistinguishable from control testes. Scale bars: 80 μm; 200 μm (insets); 30 μm (green boxes and right column).
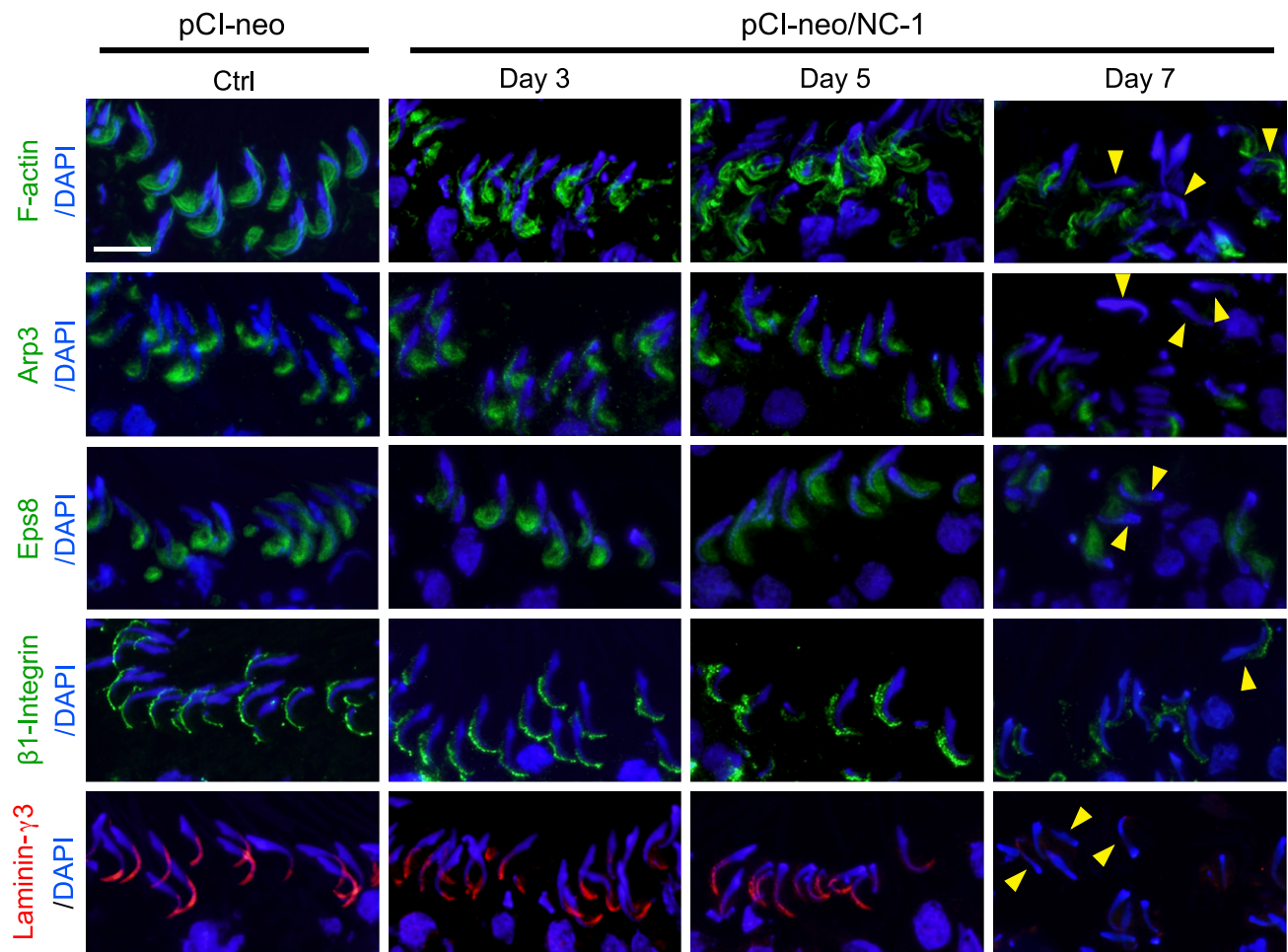
Figure 8. Overexpression of the collagen α3(IV) NC1 domain in the testis *in vivo* perturbs F-actin organization at the apical ES *via* changes in the spatial expression of actin regulatory proteins, which, in turn, alters apical ES protein distribution. Frozen sections of testes after transfection of pCI-neo/NC1 *vs.* pCI-neo (control) were stained for F-actin (green fluorescence), Arp3 (green fluorescence), and Eps8 (green fluorescence), as well as Sertoli cell–specific apical ES protein β1-integrin (green fluorescence) and spermatid-specific apical ES protein laminin-γ3 chain (red fluorescence). Cell nuclei were visualized by DAPI (blue fluorescence). F-actin was found mostly and tightly localized to the concave (ventral) side of elongated spermatid heads in stage VII tubules as bulb-like structures. By d 3 after NC1 overexpression, F-actin began to move away from the concave side of spermatid heads and became grossly mislocalized by d 5 and considerably diminished by d 7. Both Arp3 and Eps8 that tightly localized to the concave side of spermatid heads appeared as bulb-like structures in control testes. By d 3, Arp3 began to move away from the concave site, and by d 5, Arp3 staining was also detected on the convex (dorsal) side of spermatid heads (almost none in the control and found in a few spermatids by d 3). Eps8 staining seemed to diffuse away from the concave side of spermatid heads to cover the tip of spermatid heads by d 5. By d 7, localization of these 2 actin regulatory proteins was considerably diminished. These changes thus impeded the localization of 2 apical ES proteins β1-integrin as well as laminin-γ3 chain on d 5 after NC1 overexpression, and their expression was also considerably diminished by d 7. Many spermatids were found to lose their polarity. Instead of pointing toward the BM almost perpendicularly, their heads were deviated by at least 90° (yellow arrowheads) from the intended orientation. Scale bar, 20 μm.

derived peptides, such as NC1 domain, are also biologically active peptides that are capable of modulating cell adhesion function, cell apoptosis, angiogenesis, and tissue regeneration (4, 74–76). These findings thus prompted us to examine whether the NC1 domain found in collagen α3(IV) chain—one of the major building blocks of the BM in the testis—could have biologic effects similar to the other collagen chains in other epithelia and/or endothelia. If so, this will support the concept that there is a local regulatory axis between the BTB/basal ES, the apical ES, and the BM to coordinate cellular events during the epithelial cycle of spermatogenesis. This notion was also supported by the previous finding that a disruption of BM function by actively immunizing rodents with anti-BM Abs induced gross disruption of the seminiferous epithelium, which in turn compromised spermatogenesis (10, 77).

On the basis of the known sequence of rat collagen α3(IV), the NC1 domain was cloned into a mammalian expression vector pCI-neo (34), with or without a putative SP of collagen α3(IV) to assess whether its biologic effects are potentiated in the presence of an SP and to assess whether its effects are mediated *via* inside-out *vs.* outside-in signaling. These 2 NC1 domain clones were
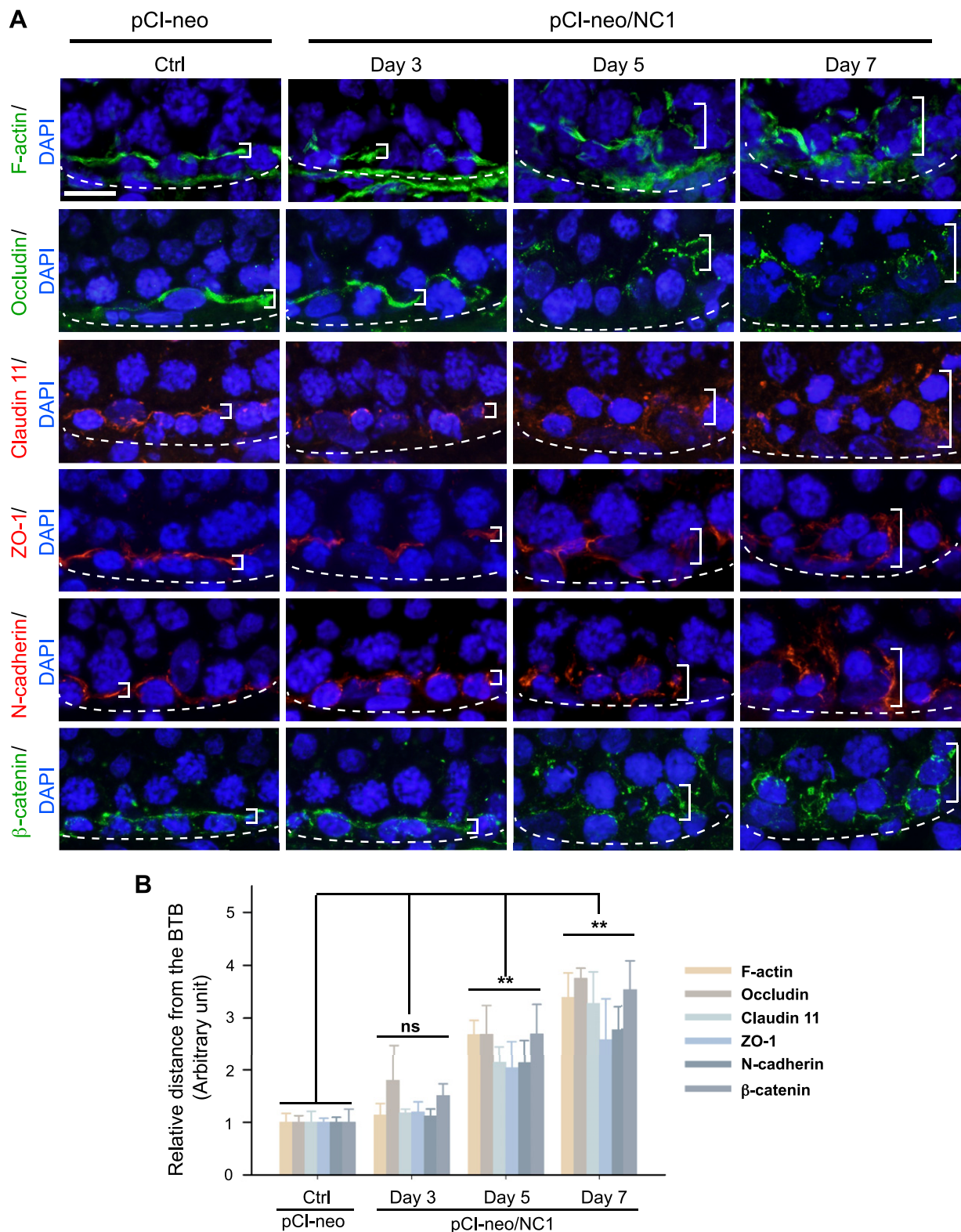
Figure 9. Overexpression of the collagen α3(IV) NC1 domain in the testis *in vivo* perturbs the organization of F-actin at the BTB, leading to mislocalization of TJ and basal ES proteins. *A*) Frozen sections of testes following transfection of pCI-neo/NC1 *vs.* pCI-neo (control) were stained for F-actin (green fluorescence), TJ proteins occludin (green), claudin 11 (red), and ZO-1 (red), as well as basal ES proteins N-cadherin (red) and β-catenin (green). Cell nuclei were visualized by DAPI (blue fluorescence) with the BM annotated by a white dashed line. After overexpression of the NC1 domain at time 0, although no obvious changes were noted by d 3, the organization of F-actin was grossly affected such that F-actin was no longer tightly packed at the BTB, but diffusely localized at the site (white brackets). As the TJ and basal ES proteins all utilized F-actin for attachment, the disruptive organization of F-actin thus impeded their localization such that they were diffused away from the BTB (annotated by the white brackets *vs.* control testes). Scale bar, 20 μm. *B*) Bar graph summarizes results shown in panel *A* from ~50 randomly selected tubules for examination, with each bar a mean ± SD of *n* = 3 rats (a total of ~150 tubules). N.s., not significant. **$P < 0.01$, Student's *t* test.

then overexpressed separately in Sertoli cells, with their overexpression confirmed by IB as reported herein. It was shown that when the collagen α3(IV) NC1 domain was overexpressed in Sertoli cell epithelium with an established functional TJ barrier, earlier shown to mimic the Sertoli cell BTB *in vivo*, it perturbed Sertoli cell TJ permeability barrier function regardless of the presence of an SP, which demonstrated that it can mediate its effects *via* inside-out signaling or outside-in signaling, consistent with earlier studies that used recombinant NC1 protein (34). Of interest, the effect by which overexpression of this NC1 domain peptide in Sertoli cells perturbed TJ permeability barrier disruption was shown to be mediated *via* changes in the localization of BTB-associated TJ and basal ES proteins. As these adhesion protein complexes all utilized F-actin for attachment, we next examined any changes in the organization of F-actin. As expected, overexpression of this NC1 domain was found to disrupt F-actin organization in Sertoli cells, wherein actin microfilaments no longer stretched across the entire Sertoli cell cytosol. Instead, they were either truncated or localized in the cellular domain close to the cell cortical zone and appeared as a branched/defragmented network. These changes apparently were the result of an alteration of the spatial expression of actin-regulatory proteins Arp3 and Eps8 in Sertoli cells. In this context, it is noted that Arp3 is known to induce barbed-end polymerization of a linear actin microfilament, thereby effectively making bundled actin filaments become a branched configuration (78). Conversely, Eps8 is an actin barbed-end capping and bundling protein that induces actin microfilaments to assume a bundled configuration (79). The combined effects of these 2 proteins thus confer F-actin its plasticity to support actin dynamics to promote cell adhesion and cell (*e.g.,* spermatid) and organelle (*e.g.,* residual body, phagosome) transport during the epithelial cycle. Of importance, similar disruptive changes on the organization of F-actin in the seminiferous epithelium were noted when the NC1 domain was overexpressed in the adult rat testis *in vivo*. In addition, MT organization was also considerably perturbed after NC1 domain overexpression in the testis, whereas the distinctive track-like structures conferred by MTs were no longer detected. As recent studies have shown that these track-like structures are important for supporting spermatid transport across the epithelium (59, 60), it is not surprising to find that many elongated spermatids remained trapped deep inside the epithelium even in tubules that had undergone NC1 domain–induced spermiation.

In short, within 3 to 5 d after overexpression of NC1 in the testis, elongated spermatids began to undergo premature spermiation in the testis in non–stage VIII tubules, such as stages VI and VII tubules. A careful examination of the distribution and/or organization of F-actin and the distribution of the apical ES proteins in the seminiferous epithelium indeed support the notion that the apical ES in the tubules undergoing premature spermiation has been compromised. This is also the result of changes in the tightly regulated spatiotemporal expression of actin regulatory proteins Arp3 and Eps8. These findings illustrate that the disruptive effects of NC1 on spermatogenesis after

its overexpression either in Sertoli cells cultured *in vitro* or in the testis *in vivo* are mediated by changes in the organization of F-actin– and MT-based cytoskeletons. These findings also support the concept that the NC1 domain peptide that is transported from the BM to the apical ES at stages VIII–IX is used to induce apical ES degeneration to facilitate the release of sperm at spermiation. In addition, the NC1 domain peptide is also used to induce BTB remodeling at these stages when preleptotene spermatocytes are transported across the immunologic barrier to develop into zygotene and pachytene spermatocytes to prepare for meiosis at stage XIV of the epithelial cycle. As such, the collagen α3(IV) NC1 domain peptide apparently serves as an autocrine factor to coordinate these events that take place at the opposite ends of the epithelium. As the seminiferous epithelium is composed of a Sertoli cell monolayer in which each Sertoli cell is responsible for the intricate development of ∼30–50 germ cells (80) at different stages of development, it is envisioned that the best mechanism with which to connect cellular events across the epithelium is *via* changes in the underlying cytoskeletal network. This concept is also supported by recent studies wherein biologically active fragments generated from laminin-γ3 chains (*e.g.,* F5-peptide) at the apical ES also utilize a similar mechanism to coordinate the remodeling of the basal ES/BTB and degeneration of the apical ES at stage VIII of the epithelial cycle (39).

The underlying mechanism by which the NC1 domain is cleaved from the collagen α3(IV) chain in the BM remains to be investigated. An earlier study has shown that this is likely mediated by TNF-α, which induces a surge in MMP9 expression (11, 61). MMP9 then mediates cleavage of collagen α3(IV) to generate the biologically active NC1 domain peptide, which is transported to the apical ES at stages VIII–IX of the epithelial cycle. This possibility must be carefully investigated in future studies. Nonetheless, we have unequivocally demonstrated the presence of a local apical ES-BTB/basal ES-BM axis that coordinates the events of spermiation and BTB remodeling mediated by the NC1 domain derived from the collagen α3(IV) chain in the BM. This functional axis is physiologically significant as it provides a new concept for the regulation of BTB during spermatogenesis. While the hypothalamic-pituitary-testis axis is important to provide the hormonal basis to support spermatogenesis, these locally produced autocrine factors are crucial to coordinate cellular events across the seminiferous epithelium during the epithelial cycle of spermatogenesis. Fj

AUTHOR CONTRIBUTIONS

REFERENCES

1. Skinner, M. K., Tung, P. S., and Fritz, I. B. (1985) Cooperativity between Sertoli cells and testicular peritubular cells in the production and deposition of extracellular matrix components. *J. Cell Biol.* **100**, 1941–1947

2. Skinner, M. K., and Fritz, I. B. (1985) Structural characterization of proteoglycans produced by testicular peritubular cells and Sertoli cells. *J. Biol. Chem.* **260**, 11874–11883

3. Dym, M. (1994) Basement membrane regulation of Sertoli cells. *Endocr. Rev.* **15**, 102–115

4. Siu, M. K. Y., and Cheng, C. Y. (2004) Dynamic cross-talk between cells and the extracellular matrix in the testis. *BioEssays* **26**, 978–992

5. Häger, M., Gawlik, K., Nyström, A., Sasaki, T., and Durbeej, M. (2005) Laminin α1 chain corrects male infertility caused by absence of laminin α2 chain. *Am. J. Pathol.* **167**, 823–833

6. Hadley, M. A., Byers, S. W., Suárez-Quian, C. A., Kleinman, H. K., and Dym, M. (1985) Extracellular matrix regulates Sertoli cell differentiation, testicular cord formation, and germ cell development *in vitro. J. Cell Biol.* **101**, 1511–1522

7. Tung, P. S., and Fritz, I. B. (1986) Extracellular matrix components and testicular peritubular cells influence the rate and pattern of Sertoli cell migration *in vitro. Dev. Biol.* **113**, 119–134

8. Tung, P. S., and Fritz, I. B. (1993) Interactions of Sertoli cells with laminin are essential to maintain integrity of the cytoskeleton and barrier functions of cells in culture in the two-chambered assembly. *J. Cell. Physiol.* **156**, 1–11

9. Lustig, L., Denduchis, B., González, N. N., and Puig, R. P. (1978) Experimental orchitis induced in rats by passive transfer of an antiserum to seminiferous tubule basement membrane. *Arch. Androl.* **1**, 333–343

10. Denduchis, B., Satz, M. L., Sztein, M. B., Puig, R. P., Doncel, G., and Lustig, L. (1985) Multifocal damage of the testis induced in rats by passive transfer of antibodies prepared against non-collagenous fraction of basement membrane. *J. Reprod. Immunol.* **7**, 59–75

11. Siu, M. K. Y., Lee, W. M., and Cheng, C. Y. (2003) The interplay of collagen IV, tumor necrosis factor-α, gelatinase B (matrix metalloprotease-9), and tissue inhibitor of metalloproteases-1 in the basal lamina regulates Sertoli cell-tight junction dynamics in the rat testis. *Endocrinology* **144**, 371–387

12. Davis, C. M., Papadopoulos, V., Sommers, C. L., Kleinman, H. K., and Dym, M. (1990) Differential expression of extracellular matrix components in rat Sertoli cells. *Biol. Reprod.* **43**, 860–869

13. Fröjdman, K., Pelliniemi, L. J., and Virtanen, I. (1998) Differential distribution of type IV collagen chains in the developing rat testis and ovary. *Differentiation* **63**, 125–130

14. Gelly, J. L., Richoux, J. P., Leheup, B. P., and Grignon, G. (1989) Immunolocalization of type IV collagen and laminin during rat gonadal morphogenesis and postnatal development of the testis and epididymis. *Histochemistry* **93**, 31–37

15. Kahsai, T. Z., Enders, G. C., Gunwar, S., Brunmark, C., Wieslander, J., Kalluri, R., Zhou, J., Noelken, M. E., and Hudson, B. G. (1997) Seminiferous tubule basement membrane. Composition and organization of type IV collagen chains, and the linkage of α3(IV) and α5(IV) chains. *J. Biol. Chem.* **272**, 17023–17032

16. Ortega, N., and Werb, Z. (2002) New functional roles for non-collagenous domains of basement membrane collagens. *J. Cell Sci.* **115**, 4201–4214

17. Sudhakar, A., and Boosani, C. S. (2008) Inhibition of tumor angiogenesis by tumstatin: insights into signaling mechanisms and implications in cancer regression. *Pharm. Res.* **25**, 2731–2739

18. Sudhakar, A., and Boosani, C. S. (2007) Signaling mechanisms of endogenous angiogenesis inhibitors derived from type IV collagen. *Gene Regul. Syst. Bio.* **1**, 217–226

19. Barczyk, M., Carracedo, S., and Gullberg, D. (2010) Integrins. *Cell Tissue Res.* **339**, 269–280

20. Mundel, T. M., Yliniemi, A. M., Maeshima, Y., Sugimoto, H., Kieran, M., and Kalluri, R. (2008) Type IV collagen α6 chain-derived non-collagenous domain 1 (α6(IV)NC1) inhibits angiogenesis and tumor growth. *Int. J. Cancer* **122**, 1738–1744

21. Maeshima, Y., Manfredi, M., Reimer, C., Holthaus, K. A., Hopfer, H., Chandamuri, B. R., Kharbanda, S., and Kalluri, R. (2001) Identification of the anti-angiogenic site within vascular basement membrane-derived tumstatin. *J. Biol. Chem.* **276**, 15240–15248

22. Maeshima, Y., Yerramalla, U. L., Dhanabal, M., Holthaus, K. A., Barbashov, S., Kharbanda, S., Reimer, C., Manfredi, M., Dickerson, W. M., and Kalluri, R. (2001) Extracellular matrix-derived peptide binds to α(v)β(3) integrin and inhibits angiogenesis. *J. Biol. Chem.* **276**, 31959–31968

23. Aikio, M., Alahuhta, I., Nurmenniemi, S., Suojanen, J., Palovuori, R., Teppo, S., Sorsa, T., López-Otín, C., Pihlajaniemi, T., Salo, T., Heljasvaara, R., and Nyberg, P. (2012) Arresten, a collagen-derived angiogenesis inhibitor, suppresses invasion of squamous cell carcinoma. *PLoS One* **7**, e51044

24. Maeshima, Y., Colorado, P. C., Torre, A., Holthaus, K. A. G., Grunkemeyer, J. A., Ericksen, M. B., Hopfer, H., Xiao, Y., Stillman, I. E., and Kalluri, R. (2000) Distinct antitumor properties of a type IV collagen domain derived from basement membrane. *J. Biol. Chem.* **275**, 21340–21348

25. Hamano, Y., Zeisberg, M., Sugimoto, H., Lively, J. C., Maeshima, Y., Yang, C., Hynes, R. O., Werb, Z., Sudhakar, A., and Kalluri, R. (2003) Physiological levels of tumstatin, a fragment of collagen IV α3 chain, are generated by MMP-9 proteolysis and suppress angiogenesis *via* alphaV β3 integrin. *Cancer Cell* **3**, 589–601

26. Hamano, Y., and Kalluri, R. (2005) Tumstatin, the NC1 domain of α3 chain of type IV collagen, is an endogenous inhibitor of pathological angiogenesis and suppresses tumor growth. *Biochem. Biophys. Res. Commun.* **333**, 292–298

27. Rehn, M., Veikkola, T., Kukk-Valdre, E., Nakamura, H., Ilmonen, M., Lombardo, C., Pihlajaniemi, T., Alitalo, K., and Vuori, K. (2001) Interaction of endostatin with integrins implicated in angiogenesis. *Proc. Natl. Acad. Sci. USA* **98**, 1024–1029

28. Pasco, S., Monboisse, J. C., and Kieffer, N. (2000) The α 3(IV)185-206 peptide from noncollagenous domain 1 of type IV collagen interacts with a novel binding site on the β 3 subunit of integrin α Vbeta 3 and stimulates focal adhesion kinase and phosphatidylinositol 3-kinase phosphorylation. *J. Biol. Chem.* **275**, 32999–33007

29. Kamphaus, G. D., Colorado, P. C., Panka, D. J., Hopfer, H., Ramchandran, R., Torre, A., Maeshima, Y., Mier, J. W., Sukhatme, V. P., and Kalluri, R. (2000) Canstatin, a novel matrix-derived inhibitor of angiogenesis and tumor growth. *J. Biol. Chem.* **275**, 1209–1215

30. Le Magueresse-Battistoni, B., Morera, A. M., and Benahmed, M. (1995) *In vitro* regulation of rat Sertoli cell inhibin messenger RNA levels by transforming growth factor-β 1 and tumour necrosis factor α. *J. Endocrinol.* **146**, 501–508

31. Mruk, D. D., and Cheng, C. Y. (2011) An *in vitro* system to study Sertoli cell blood-testis barrier dynamics. *Methods Mol. Biol.* **763**, 237–252

32. Gao, Y., Mruk, D., Chen, H., Lui, W. Y., Lee, W. M., and Cheng, C. Y. (2017) Regulation of the blood-testis barrier by a local axis in the testis: role of laminin α2 in the basement membrane. *FASEB J.* **31**, 584–597

33. Russell, L. D., Saxena, N. K., and Turner, T. T. (1989) Cytoskeletal involvement in spermiation and sperm transport. *Tissue Cell* **21**, 361–379

34. Wong, E. W., and Cheng, C. Y. (2013) NC1 domain of collagen α3(IV) derived from the basement membrane regulates Sertoli cell blood-testis barrier dynamics. *Spermatogenesis* **3**, e25465

35. Chen, H., Mruk, D. D., Lee, W. M., and Cheng, C. Y. (2016) Planar cell polarity (PCP) protein Vangl2 regulates ectoplasmic specialization dynamics *via* its effects on actin microfilaments in the testes of male rats. *Endocrinology* **157**, 2140–2159

36. Wan, H. T., Mruk, D. D., Li, S. Y., Mok, K. W., Lee, W. M., Wong, C. K., and Cheng, C. Y. (2013) p-FAK-Tyr(397) regulates spermatid adhesion in the rat testis *via* its effects on F-actin organization at the ectoplasmic specialization. *Am. J. Physiol. Endocrinol. Metab.* **305**, E687–E699

37. Zwain, I. H., and Cheng, C. Y. (1994) Rat seminiferous tubular culture medium contains a biological factor that inhibits Leydig cell steroidogenesis: its purification and mechanism of action. *Mol. Cell. Endocrinol.* **104**, 213–227

38. Lee, N. P. Y., Mruk, D., Lee, W. M., and Cheng, C. Y. (2003) Is the cadherin/catenin complex a functional unit of cell-cell actin-based adherens junctions in the rat testis? *Biol. Reprod.* **68**, 489–508

39. Gao, Y., Mruk, D. D., Lui, W. Y., Lee, W. M., and Cheng, C. Y. (2016) F5-peptide induces aspermatogenesis by disrupting organization of actin- and microtubule-based cytoskeletons in the testis. *Oncotarget* **7**, 64203–64220

40. Furuse, M., Hata, M., Furuse, K., Yoshida, Y., Haratake, A., Sugitani, Y., Noda, T., Kubo, A., and Tsukita, S. (2002) Claudin-based tight junctions are crucial for the mammalian epidermal barrier: a lesson from claudin-1-deficient mice. *J. Cell Biol.* **156**, 1099–1111

41. Chen, Y., Merzdorf, C., Paul, D. L., and Goodenough, D. A. (1997) COOH terminus of occludin is required for tight junction barrier function in early *Xenopus* embryos. *J. Cell Biol.* **138**, 891–899

42. Wong, C. H., Mruk, D. D., Lui, W. Y., and Cheng, C. Y. (2004) Regulation of blood-testis barrier dynamics: an *in vivo* study. *J. Cell Sci.* **117**, 783–798

43. Hew, K. W., Heath, G. L., Jiwa, A. H., and Welsh, M. J. (1993) Cadmium *in vivo* causes disruption of tight junction-associated microfilaments in rat Sertoli cells. *Biol. Reprod.* **49**, 840–849

44. Xiao, X., Wong, E. W. P., Lie, P. P. Y., Mruk, D. D., Wong, C. K. C., and Cheng, C. Y. (2014) Cytokines, polarity proteins, and endosomal protein trafficking and signaling-the Sertoli cell blood-testis barrier system *in vitro* as a study model. *Methods Enzymol.* **534**, 181–194

45. Xiao, X., Mruk, D. D., Wong, E. W. P., Lee, W. M., Han, D., Wong, C. K. C., and Cheng, C. Y. (2014) Differential effects of c-Src and c-Yes on the endocytic vesicle-mediated trafficking events at the Sertoli cell blood-testis barrier: an *in vitro* study. *Am. J. Physiol. Endocrinol. Metab.* **307**, E553–E562

46. Ip, C. K., Cheung, A. N., Ngan, H. Y., and Wong, A. S. (2011) p70 S6 kinase in the control of actin cytoskeleton dynamics and directed migration of ovarian cancer cells. *Oncogene* **30**, 2420–2432

47. Mok, K. W., Chen, H., Lee, W. M., and Cheng, C. Y. (2015) rpS6 regulates blood-testis barrier dynamics through Arp3-mediated actin microfilament organization in rat sertoli cells. An *in vitro* study. *Endocrinology* **156**, 1900–1913

48. Xiao, X., Mruk, D. D., Tang, E. I., Massarwa, R., Mok, K. W., Li, N., Wong, C. K., Lee, W. M., Snapper, S. B., Shilo, B. Z., Schejter, E. D., and Cheng, C. Y. (2014) N-wasp is required for structural integrity of the blood-testis barrier. *PLoS Genet.* **10**, e1004447

49. Pizarro-Cerda, J., Chorev, D. S., Geiger, B., and Cossart, P. (2016) The diverse family of Arp2/3 complexes. *Trends Cell Biol.* **27**, 93–100

50. Cheng, C. Y., and Mruk, D. D. (2011) Regulation of spermiogenesis, spermiation and blood-testis barrier dynamics: novel insights from studies on Eps8 and Arp3. *Biochem. J.* **435**, 553–562

51. Palombi, F., Salanova, M., Tarone, G., Farini, D., and Stefanini, M. (1992) Distribution of β 1 integrin subunit in rat seminiferous epithelium. *Biol. Reprod.* **47**, 1173–1182

52. Ozaki-Kuroda, K., Nakanishi, H., Ohta, H., Tanaka, H., Kurihara, H., Mueller, S., Irie, K., Ikeda, W., Sakai, T., Wimmer, E., Nishimune, Y., and Takai, Y. (2002) Nectin couples cell-cell adhesion and the actin scaffold at heterotypic testicular junctions. *Curr. Biol.* **12**, 1145–1150

53. Walia, A., Yang, J. F., Huang, Y. H., Rosenblatt, M. I., Chang, J. H., and Azar, D. T. (2015) Endostatin's emerging roles in angiogenesis, lymphangiogenesis, disease, and clinical applications. *Biochim. Biophys. Acta* **1850**, 2422–2438

54. Shen, B., Delaney, M. K., and Du, X. (2012) Inside-out, outside-in, and inside-outside-in: G protein signaling in integrin-mediated cell adhesion, spreading, and retraction. *Curr. Opin. Cell Biol.* **24**, 600–606

55. Hu, P., and Luo, B. H. (2013) Integrin bi-directional signaling across the plasma membrane. *J. Cell. Physiol.* **228**, 306–312

56. Siu, M. K. Y., Wong, C. H., Lee, W. M., and Cheng, C. Y. (2005) Sertoli-germ cell anchoring junction dynamics in the testis are regulated by an interplay of lipid and protein kinases. *J. Biol. Chem.* **280**, 25029–25047

57. Li, M. W. M., Mruk, D. D., Lee, W. M., and Cheng, C. Y. (2009) Disruption of the blood-testis barrier integrity by bisphenol A *in vitro*: is this a suitable model for studying blood-testis barrier dynamics? *Int. J. Biochem. Cell Biol.* **41**, 2302–2314

58. Ma, Y., Yang, H. Z., Xu, L. M., Huang, Y. R., Dai, H. L., and Kang, X. N. (2015) Testosterone regulates the autophagic clearance of androgen binding protein in rat Sertoli cells. *Sci. Rep.* **5**, 8894

59. Tang, E. I., Lee, W. M., and Cheng, C. Y. (2016) Coordination of actin- and microtubule-based cytoskeletons supports transport of spermatids and residual bodies/phagosomes during spermatogenesis in the rat testis. *Endocrinology* **157**, 1644–1659

60. Li, N., Mruk, D. D., Tang, E. I., Lee, W. M., Wong, C. K., and Cheng, C. Y. (2016) Formin 1 regulates microtubule and F-actin organization to support spermatid transport during spermatogenesis in the rat testis. *Endocrinology* **157**, 2894–2908

61. Siu, M. K. Y., and Cheng, C. Y. (2004) Interactions of proteases, protease inhibitors, and the β1 integrin/laminin γ3 protein complex in the regulation of ectoplasmic specialization dynamics in the rat testis. *Biol. Reprod.* **70**, 945–964

62. Yan, H. H. N., and Cheng, C. Y. (2006) Laminin α 3 forms a complex with β3 and γ3 chains that serves as the ligand for α 6β1-integrin at the apical ectoplasmic specialization in adult rat testes. *J. Biol. Chem.* **281**, 17286–17303

63. Vogl, A. W., Vaid, K. S., and Guttman, J. A. (2008) The Sertoli cell cytoskeleton. *Adv. Exp. Med. Biol.* **636**, 186–211

64. Cheng, C. Y., and Mruk, D. D. (2010) A local autocrine axis in the testes that regulates spermatogenesis. *Nat. Rev. Endocrinol.* **6**, 380–395

65. Cheng, C. Y., and Mruk, D. D. (2012) The blood-testis barrier and its implications for male contraception. *Pharmacol. Rev.* **64**, 16–64

66. Pelletier, R. M. (2011) The blood-testis barrier: the junctional permeability, the proteins and the lipids. *Prog. Histochem. Cytochem.* **46**, 49–127

67. Schlatt, S., and Ehmcke, J. (2014) Regulation of spermatogenesis: an evolutionary biologist's perspective. *Semin. Cell Dev. Biol.* **29**, 2–16

68. O'Donnell, L., Nicholls, P. K., O'Bryan, M. K., McLachlan, R. I., and Stanton, P. G. (2011) Spermiation: the process of sperm release. *Spermatogenesis* **1**, 14–35

69. Winters, S. J., and Moore, J. P. (2004) Intra-pituitary regulation of gonadotrophs in male rodents and primates. *Reproduction* **128**, 13–23

70. McLachlan, R. I., O'Donnell, L., Meachem, S. J., Stanton, P. G., de, K., Pratis, K., and Robertson, D. M. (2002) Hormonal regulation of spermatogenesis in primates and man: insights for development of the male hormonal contraceptive. *J. Androl.* **23**, 149–162

71. Yan, H. H. N., Mruk, D. D., Wong, E. W. P., Lee, W. M., and Cheng, C. Y. (2008) An autocrine axis in the testis that coordinates spermiation and blood-testis barrier restructuring during spermatogenesis. *Proc. Natl. Acad. Sci. USA* **105**, 8950–8955

72. Su, L., Mruk, D. D., Lie, P. P. Y., Silvestrini, B., and Cheng, C. Y. (2012) A peptide derived from laminin-α3 reversibly impairs spermatogenesis in rats. *Nat Commun.* **3**, 1185

73. Cheng, C. Y., and Mruk, D. D. (2009) An intracellular trafficking pathway in the seminiferous epithelium regulating spermatogenesis: a biochemical and molecular perspective. *Crit. Rev. Biochem. Mol. Biol.* **44**, 245–263

74. Poluzzi, C., Iozzo, R. V., and Schaefer, L. (2016) Endostatin and endorepellin: a common route of action for similar angiostatic cancer avengers. *Adv. Drug Deliv. Rev.* **97**, 156–173

75. Cooke, V. G., and Kalluri, R. (2008) Chapter 1. Molecular mechanism of type IV collagen-derived endogenous inhibitors of angiogenesis. *Methods Enzymol.* **444**, 1–19

76. Marneros, A. G., and Olsen, B. R. (2001) The role of collagen-derived proteolytic fragments in angiogenesis. *Matrix Biol.* **20**, 337–345

77. Lustig, L., Denduchis, B., Ponzio, R., Lauzon, M., and Pelletier, R. M. (2000) Passive immunization with anti-laminin immunoglobulin G modifies the integrity of the seminiferous epithelium and induces arrest of spermatogenesis in the guinea pig. *Biol. Reprod.* **62**, 1505–1514

78. Pizarro-Cerdá, J., Chorev, D. S., Geiger, B., and Cossart, P. (2017) The diverse family of Arp2/3 complexes. *Trends Cell Biol.* **27**, 93–100

79. Ahmed, S., Goh, W. I., and Bu, W. (2010) I-BAR domains, IRSp53 and filopodium formation. *Semin. Cell Dev. Biol.* **21**, 350–356

80. Weber, J. E., Russell, L. D., Wong, V., and Peterson, R. N. (1983) Three-dimensional reconstruction of a rat stage V Sertoli cell: II. Morphometry of Sertoli–Sertoli and Sertoli–germ-cell relationships. *Am. J. Anat.* **167**, 163–179